Developing a diagnostic assay for *Pneumocystis jirovecii* pneumonia

and

Investigating the interaction of *Pneumocystis murina* and respiratory syncytial virus during co-infection in mice

By

Elizabeth D.V. Hlagala

HLGELI001

SUBMITTED TO THE UNIVERSITY OF CAPE TOWN in fulfilment of the requirements of the degree MSc (Med) Clinical Sciences and Immunology, Faculty of Health Sciences, UNIVERSITY OF CAPE TOWN

February 2025

Associate Professor J. Claire Hoving

Dr Lucian Duvenage and Professor Christopher Thornton

Declaration

I, …Elizabeth Hlagala....., hereby declare that the work on which this dissertation/thesis is based is my original work (except where acknowledgements indicate otherwise) and that neither the whole work nor any part of it has been, is being, or is to be submitted for another degree in this or any other university. I empower the university to reproduce for the purpose of research either the whole or any portion of the contents in any manner whatsoever.

Signature: …Signed by candidate…

Date: ……2025/06/16…….

Acknowledgements

The success of this project would not have been achievable without the invaluable support of my supervisors: A/P J. Claire Hoving, Dr Lucian Duvenage, and Professor Chris Thornton. I am profoundly thankful to my supervisors for their warm welcome into their lab and for believing in me despite my initial lack of experience. I could not have wished for a more supportive supervisory team. A special thanks to my primary supervisor, A/P Claire Hoving, for allowing me the space to develop and learn at my own pace, for trusting me with this project, and for encouraging me to present even when I doubted my readiness. Your kindness, understanding, and willingness to share your expertise have been instrumental, along with your support in securing funding. To my co-supervisor, Lucian, your patient and graceful teaching has been pivotal in my journey. You have consistently provided guidance and support over the past two years, helping me navigate lab work, presentations, paperwork, and various challenges with such grace while allowing me the freedom to learn from my mistakes. I am incredibly grateful for everything, from teaching me how to use a pipette to the writing process. I could not have asked for a more exceptional co-supervisor, and I cannot thank you enough for bringing ease into this journey. My appreciation also extends to Professor Chris Thornton for supplying the antiserum and offering valuable guidance on this project. I am also grateful to Rodney Lucas for training me and instilling confidence in my ability to work with mice, and to the animal unit staff for their assistance in caring for my mice.

To my family, thank you for your unwavering support during my academic journey, for being my greatest cheerleader, and for sharing in my excitement and anxieties, even when the details were unclear to you. Your encouragement has meant the world to me. I also want to express my gratitude to my friends for being there through both laughter and tears.

Abbreviations

AMs – Alveolar macrophages

APCs -Antigen-presenting cells

BAL- Bronchoalveolar lavage

CARD9- Caspase recruitment domain-containing protein 9

cART- combined antiretroviral therapy

CLCs- C-type Lectin receptors

DCs- Dendritic cells

GM-CSF- Granulocyte-macrophage colony-stimulating factor

GMS- Grocott's methenamine silver stain

HIV- Human Immunodeficiency Virus

IFN- Interferon

Ig- Immunoglobulin

IL- Interleukin

IS- Induced sputum

NF-κB-Nuclear factor Kappa B

NOD- Nucleotide-binding oligomerisation domain

MAPK- Mitogen-activated protein kinase

MHC II- Major histocompatibility complex II

M1 – Classical macrophages

M2- Alternative macrophages

MSG- Major surface glycoprotein

mtLSU-Mitochondrial large-subunit RNA gene

MyD88- Myeloid differentiation factor 88

PAMPS- Pathogen Associated Molecular Patterns

PCP- *Pneumocystis* pneumonia

PCR- Polymerase chain reaction

RLRS- Retinoic inducible receptors

ROS- Reactive oxygen species

RSV- Respiratory syncytial virus

SYK-spleen tyrosine kinase

TB -Tuberculosis

TBO- Toluidine blue o

Th- T helper

TLRs- Toll-like Receptors

TNFα- Tumour necrosis factor-alpha

Abstract

Pneumocystis pneumonia (PCP) is an AIDS-defining illness that is caused by an opportunistic fungal pathogen, *Pneumocystis jirovecii.* In immunocompromised individuals, *P. jirovecii* can result in fatal pneumonia, and healthy individuals can be reservoirs for *P. jirovecii*. PCP places a significant strain on the healthcare system, resulting in high rates of mortality and morbidity. Diagnosis of PCP remains a challenge since *Pneumocystis* species cannot reliably be cultured *in vitro.* The current methods of diagnosis are invasive, expensive, lack specificity and sensitivity and are not readily available in low-resource settings. To reduce the burden of disease, a reliable diagnostic test is necessary. Additionally, co-infections are common, especially in immunocompromised individuals, and are often linked to increased severity. In the Drakenstein Child Health Study, respiratory syncytial virus (RSV) was the most prevalent cause of pneumonia in children under 5 years. Furthermore, seroprevalence studies reveal that the majority of children under 4 years would have been exposed to *P. jirovecii*, suggesting that exposure to both organisms occur simultaneously. The interaction between RSV and *P. jirovecii* and the associated effect on mediating cross-protective effects on host immunity remain poorly understood.

In this study, we evaluated a polyclonal antibody (pAb) raised against a putative *Pneumocystis* biomarker (Kex1), with the aim of developing a lateral-flow assay (LFA) for rapid point-of-care diagnosis of PCP. Kex1 is an antigenically stable serine protease highly conserved across *Pneumocystis* species. Proof-of-principle experiments investigated the presence of Kex1 in mice experimentally infected with *P. murina* using pAb-based immunoassays. Protein samples from naïve and infected mouse lungs were analysed using Western blot and dot blot to confirm the presence of Kex1. Using the pAb at a dilution of 1/20,000, a protein of approximately 100 kDa was detected in the infected lung and serum samples, but not in naïve samples. Lastly, using a mouse model of *P. murina* and RSV coinfection, we investigated the effects of *P. murina* on viral pneumonia. Wild-type and immunocompromised RAG-1-deficient mice were infected with *P. murina* followed by RSV and the disease parameters were investigated. RT-qPCR analysis demonstrated that *P. murina* infection reduced RSV burden in coinfected mice compared to RSV-only mice. Pro-inflammatory cytokines IL-1β, IL-12 p40, IL12-p70, and IFN-γ and serum IgM and IgG levels were elevated in the *P. murina* group compared to the RSV group. Interestingly, the levels of IFN-β were significantly reduced in the coinfected group compared to the RSV group.

The detection of Kex1 in infected mouse lungs, urine, and serum of *P. murina*-infected mice makes it a promising tool for the rapid diagnosis of PCP. Urine and serum offer less invasive and inexpensive methods of diagnosing PCP. *Pneumocystis murina* reduces the burden of

RSV during coinfection in both Wild-type and RAG-1-deficient mice. This may be due to the increased pro-inflammatory response, mucus production, and antibody response during primary *P. murina* infection, which primes the immune system towards a T-helper type-2 immune response against RSV. The observed decrease in IFN-β levels in the coinfected group suggests that the reduced RSV burden may not be solely a consequence of antiviral cytokines, but rather the result of other immune mediators activated during the primary *P. murina* infection.

Keywords: *P. jirovecii*, *P. murina*, Kex-1, polyclonal antiserum, lateral flow assay, RSV, coinfection

Contents

List of Figures

1. Literature review

1.1 Epidemiology of fungal infections

It is estimated that fungal diseases are responsible for more than 2.5 million deaths annually (Denning, 2024). Nevertheless, precise global incidence estimates for fungal infections remain scarce. This is complicated by the lack of reliable diagnostic tools and the absence of comprehensive national surveillance systems (Brown et al., 2012). The global burden of invasive fungal infections is estimated to be 6.5 million people per year (McMullan et al., 2024). In Africa, the primary drivers of invasive fungal infections include human immunodeficiency virus (HIV), tuberculosis, and poverty (Bongomin et al., 2022).The following fungal pathogens are the main causative agents of severe fungal diseases: *Aspergillus*, *Cryptococcus*, *Pneumocystis jirovecii*, and *Histoplasma capsulatum* (Bongomin et al., 2017).

1.2 *Pneumocystis* Pneumonia

Pneumocystis jirovecii is an opportunistic fungal pathogen causing *Pneumocystis* pneumonia (PCP) in immunocompromised individuals, an interstitial lung disease frequently leading to life-threatening respiratory failure. In immunocompromised hosts, this pathogen can cause fatal interstitial pneumonia (Hänsel et al., 2023), while immunocompetent individuals often present with a mild respiratory infection. *Pneumocystis* spp. colonisation and PCP are associated with permanent obstructive lung damage, while colonisation is also a factor in the development of chronic obstructive pulmonary disease. *Pneumocystis* pneumonia is a comorbidity factor in patients with chronic diseases, ranking first among the AIDS-defining fungal illnesses (Tomás and Matos (2018);Guegan and Robert-Gangneux (2019)). Seroprevalence studies involving anti-*Pneumocystis* IgG have demonstrated that by the age of 4, two-thirds of children would have acquired antibodies to *P. jirovecii* (Pifer et al. (1978); Morris and Norris (2012)). Nonetheless, challenges persist in diagnosing *P. jirovecii*, primarily due to the lack of sensitive, non-invasive, reliable serological assays for *P. jirovecii* infection or colonisation.

The global prevalence of *P. jiovecii* is estimated to be >400,000 annual cases worldwide (Bongomin et al., 2017), with mortality rates ranging between 5% to 30% in HIV-infected individuals, and 4% to 76% in non-HIV immunocompromised individuals (McMullan et al., 2024). PCP is acknowledged as a significant etiological factor in the development of pneumonia in regions with a high prevalence of HIV and tuberculosis, as well as in low-income

settings. The frequency of PCP reports has increased in parallel with the rise of HIV/AIDS. The advent of combined antiretroviral therapy (cART) has been associated with a notable reduction in the incidence of PCP. Nevertheless, in resource-limited settings with a high prevalence of HIV infection and restricted access to cART, PCP infections remain a significant concern. Comorbidities have remained high in individuals who are not responding to cART treatment, and those who are unaware of their HIV status (Stringer, 2002). Furthermore, there has been an observed re-emergence in the incidence of PCP in non-HIV immunocompromised patients globally, including USA, Europe and the UK (Wang et al., 2021). This is attributed to the increased use of immunosuppressive medications and corticosteroids (Carmona and Limper, 2011). Those at risk of PCP include individuals with obesity, patients undergoing chemotherapy, and organ transplant recipients (Pates et al., 2023). While there was a global effort to combat the burden of diseases during the AIDS epidemic, this effort has since declined with the introduction of cART. The World Health Organisation recently released a fungal pathogen priority list, with *P. jirovecii* being among the medium-priority pathogens, but with a higher priority ranking for public health significance due to the lack of reliable and accessible rapid points of care of diagnosis (McMullan et al., 2024)

1.3 *Pneumocystis* Species

Sequence analysis has revealed that the *Pneumocystis* genus is a group of atypical fungi, that have co-evolved to become host specific. These include the previously mentioned *P. jirovecii* that infects humans; *P. carinii* in rats; *P. murina* in mice; and *P. oryctolagus* in rabbits (Ma et al., 2018). Furthermore, *Pneumocystis* has lost a significant number of genes required for survival and has become completely dependent on the host for survival, known as obligate biotrophy. Several metabolic pathways and cell wall components have been removed or replaced with the most notable being ergosterol, which has been replaced by cholesterol (Joffrion and Cushion (2010); Ma et al. (2018)). Consequently, *Pneumocystis* is resistant to antifungals that target ergosterol (Aliouat-Denis et al., 2008).

Pneumocystis infects the host to colonise the lungs where it replicates through a series of life cycle stages (see Fig 1). The lungs are the primary site of *Pneumocystis* infection, where the organism exists almost exclusively in the alveoli. Although rare, extrapulmonary sites of *Pneumocystis* have been reported in severely immunocompromised individuals. These include but are not limited to, the kidneys, brain, spleen, gastrointestinal tract, pericardium, liver, bone marrow, and blood vessels (Ng et al., 1997). *Pneumocystis* attaches to Type 1 pneumocytes in the lungs using extracellular matrix proteins (Gigliotti et al., 2014). *Pneumocystis* exists in three forms: the trophic, cystic (asci), and sporozoite forms. The trophic form represents 90-95% of the life cycle stages, making it the most abundant in the

lungs (Aliouat-Denis et al., 2009). This form is highly pleomorphic, varying in sizes of less than 10μm, with a thin flexible cell wall and a single haploid nucleus (Walzer (2001); Skalski et al. (2015)). On the surface, there are cytoplasmic projections termed filopodia, which protrude towards the host cell to penetrate invaginations (Apostolopoulou and Fishman, 2022). These cytoplasmic projections are hypothesised to play a role in nutrient uptake. Trophs also express major surface glycoproteins (MSG) on their surface which is important during the host immune response (Wang et al., 2023). The cystic forms are spherical in shape, and have a thick, smooth cell wall composed of β(1,3)-glucan, a complex branching polysaccharide containing other proteins (Carmona and Limper, 2011). Cysts also contain 8 intracystic bodies that rupture to become trophs. Like the MSGs found in trophs, β(1,3)-glucan is also important during the host's innate immune response. While the trophozoite is the active, replicating, infective form, the cysts are the dormant stage that allows the fungus to survive in the extrapulmonary environment (Ma et al., 2018).

Transmission occurs through the inhalation of cysts in the air, which are the only forms that are able to live in the external environment (Islam et al., 2023). Infection occurs when the trophozoite form attaches and tightly adheres to Type I pneumocytes (Hoving et al., 2023), using filopodia. In the lungs, the life cycle is biphasic and comprises two distinct phases: the asexual phase, in which the trophozoites divide by binary fission, and the sexual phase, in which the trophozoites conjugate to form early sporozoites (Kelly and Shellito, 2010). The early sporozoites undergo a series of meiotic and mitotic divisions to mature into sporozoites with eight nucleic spores. Subsequently, the spores develop into thick-walled cysts (Apostolopoulou and Fishman, 2022). The thick walls of cysts are composed of β(1,3)-glucan, which is recognised by alveolar macrophages, lung epithelial cells, and dendritic cells, which prime a T-cell response (Hoving and Kolls, 2017).

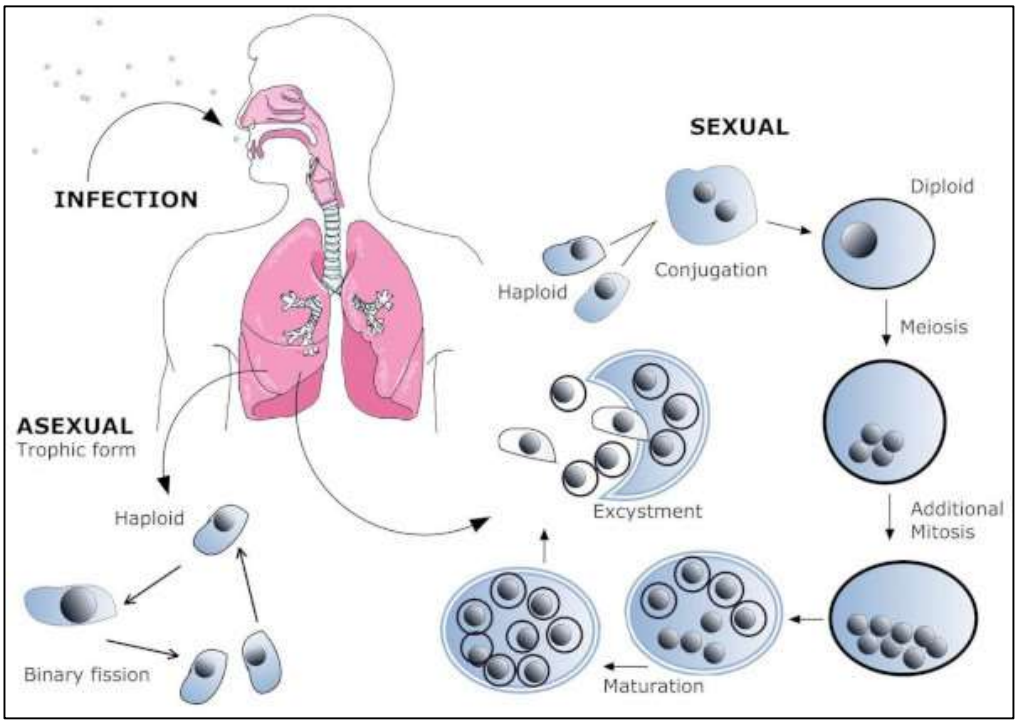

Figure 1: Proposed life cycle of *Pneumocystis* species

Cystic and trophic forms define the life cycle in a mammalian host. The inhaled cysts release 8 haploid trophs that conjugate sexually or divide by binary fission asexually to form mature cysts. The trophs are the predominant form that colonises the lung (Beck and Cushion, 2009)

1.4 Symptoms and Diagnosis

The signs and symptoms of PCP are often nonspecific (Esteves et al., 2015) thus making the diagnosis of PCP difficult. The common symptoms include fever, non-reproductive cough and dyspnoea, with normal lung exams (Bateman et al., 2020). Diagnosis of the diseases, therefore, depends on a combination of nonspecific clinical assessments, arterial blood gas, pulmonary function, radiological testing and laboratory tests (Tomás and Matos, 2018). Radiological features often reveal bilateral perihilar interstitial infiltrates and increased involvement of the lung fields (Bateman et al., 2020). A blood gas analysis indicates a state of hypoxemia and a partial pressure of oxygen (PaO2) in the peripheral blood of ≤ 9.3 kPa (70 mmHg) (Tomás and Matos, 2018).

1.5 Diagnosis by molecular techniques, staining and microscopy

Current methods of diagnosis use biological samples from the lower respiratory tract. These include bronchoalveolar lavage (BAL), induced sputum, endobronchial biopsies, bronchial excretions, and transbronchial biopsies (Tomás and Matos, 2018). Biopsies present a number

of disadvantages, including invasiveness and difficulty in collection in patients who have reached the end stage of the disease, those experiencing respiratory failure, children, and those in low-resource settings (Tomás and Matos, 2018). Alternative samples that have been considered for the detection of *P. jirovecii* include oral washes, nasopharyngeal aspirates, blood serum, and urine. Molecular methods, including reverse transcription-quantitative polymerase chain reaction (RT-qPCR), nested polymerase chain reaction (nPCR), antigen-antibody assays, and loop-mediated isothermal amplification, are applied to respiratory samples for the detection of infection ((Tomás and Matos (2018); Bateman et al. (2020)).

Bronchoalveolar lavage fluid is the current gold standard for PCP diagnosis because of the high quality of respiratory samples. However, BAL presents many disadvantages in that it is invasive, expensive and unsafe in patients with severe pulmonary diseases (Bateman et al., 2020). The samples from sputum are used for immunofluorescent staining and PCR, which has high sensitivity (Lipschik et al., 1992). Most PCR assays use primers from mitochondrial large-subunit RNA gene (mtLSU) or the MSG family of genes (Ma et al., 2018). When compared to nPCR, RT-qPCR has greater sensitivity and specificity; between 94-99% and 89-96% respectively (Tomás and Matos, 2018). In an effort to use less invasive methods, Larsen et al. (2004) conducted a study using oral washes which were subsequently used for PCR. Here, the sensitivity and specificity were 88% and 85% respectively (Larsen et al., 2004).

Diagnosis of PCP also relies on microscopic visualisation, in which histological samples are stained and imaged. The cell wall of the cysts is stained by the following stains: Giemsa, Wright stains, Diffuse quick, Gomori-methenamine-silver (GMS) or DQ, Gram-Weigert, Toluidine Blue O, Crystal violet, and Calcofluor white stain (Bateman et al., 2020). Immunofluorescent staining stains both the cyst and trophozoite forms, and it uses direct fluorescent antibodies with monoclonal antibodies (mAb) to detect *Pneumocystis* antigens (Choe et al. (2014); Tomás and Matos (2018); Truong and Ashurst (2023)). When comparing the sensitivity and specificity, immunofluorescent staining has the highest sensitivity (97%) when used on bronchoalveolar lavage fluid (BAL) samples. Toluidine blue combined with immunofluorescence staining has been demonstrated to achieve the highest level of sensitivity, reaching 100% when staining is conducted on BAL samples (Tomás and Matos, 2018). These methods require a high level of expertise and the use of specialised equipment. Therefore, it is imperative to develop alternative, non-invasive and inexpensive methods of detection.

1.6 Biomarkers

Seroprevalence studies have investigated the presence of different biomarkers in the serum of PCP patients. These biomarkers include β(1,3)-glucan, lactate dehydrogenase (LH), Krebs

von den lungen-6 Antigen (KL-6), S-adenosyl methionine (SAM) and surfactant protein D (Esteves et al. (2015); Tomás and Matos (2018)). The serological tests of these metabolites have been demonstrated to be of limited utility, exhibiting low sensitivity and specificity for *P. jirovecii*. This increases the likelihood of false positives during diagnosis (Tomás et al., 2016). β(1,3)-glucan is a cell wall polysaccharide present in the majority of fungal species, including *P. jirovecii*. The assay to detect β(1,3)-glucan demonstrates a high sensitivity (91%), and when combined with LDH or KL-6, the sensitivity and specificity increase to 97% and 94%, respectively (Tomás and Matos, 2018). Levels of β(1,3)-glucan have been reported to be elevated in patients with PCP, but the diagnostic value of this marker has remained uncertain.β(1,3)-glucan testing has a low specificity of 77% (Tomás and Matos, 2018). A positive test could therefore be an indication of other fungal infections such as aspergillosis, candidiasis, and fusariosis (Bateman et al. (2020); Del Corpo et al. (2020)). A previous study revealed that when the cut-off limit for β(1,3)-glucan was set at 100 pg/ml, the levels of LDH and β(1,3)-glucan were promising tools for the diagnosis of PCP when used concurrently (Esteves et al., 2014). The rationale for using SAM in serum assays was that *Pneumocystis* has lost the metabolic pathway synthesising SAM and must thus scavenge it from its host. S-adenosyl methionine is a crucial biochemical intermediate in methylation reactions and polyamine synthesis. Patients with PCP would thus be expected to have reduced levels of SAM (Huang et al., 2011).

Increased knowledge of the role of humoral immunity in PCP has rendered the use of serum antibodies an alternative tool for the diagnosis of PCP (Tomás et al., 2020). The most extensively investigated antigens in seroprevalence studies are those belonging to the MSG and Kexin (Kex1) groups (Pungan et al., 2023). Major surface glycoproteins are a family of genes that encode surface glycoproteins, which *Pneumocystis* uses to evade the host's defence mechanisms and adhere to host cells during different stages of its life cycle (Gingo et al., 2011).These proteins contain protective epitopes and are highly immunogenic (Djawe et al., 2010). The recombinant segments of MSG such as MsgA, B, and C have been used to study the humoral response to *Pneumocystis*, with MsgC being the most strongly recognised by serum antibodies of HIV-infected individuals who have recovered from PCP (Gingo et al., 2011). However, the multiple epitopes on MSG allow for antigenic variation, making it an unreliable maker for diagnosis. MSG isoforms differ by *Pneumocystis* species, contributing to host specificity and evasion (Gigliotti et al., 2014). Thus, antibodies against MSG can cross-react with epitopes of similar size from other *Pneumocystis* species (Schaffzin et al., 1999). Previous MSG based ELISA's have shown low sensitivities and specificities of 68% and 61.8%, respectively (Tomás et al., 2016).

Kex1 is an antigenically stable serine *Pneumocystis* protease coded by a single nuclear copy gene, PRT1 (Kutty and Kovacs, 2003). These properties make it interesting in the diagnosis of *Pneumocystis* as it avoids genetic mutation, making it conserved across *Pneumocystis* species. It is hypothesised that Kex1 is involved in the proteolytic processing of *Pneumocystis* major surface antigens as well as the processing of proteins in the Golgi apparatus (Morris and Norris, 2012). In HIV-infected simians, it was observed that the antibody responses to Kex1 were detected with the onset of *Pneumocystis* colonisation, while low Kex1 titres before immunosuppression predicted the development of *Pneumocystis* colonisation (Kling et al., 2010). Both the non-human primate studies and rodent studies support the preventative role of Kex1 antibodies (Gigliotti et al. (2002); Kling et al. (2010)). Monoclonal antibodies against Kex1 have been shown to confer protection against PCP and these antibodies can recognise antigens from *Pneumocystis* spp. from other mammalian hosts such as ferrets, humans, and rhesus macaques (Cobos Jiménez et al., 2019). In a recent study, Tomás et al. (2020) developed an ELISA for Kex1 to detect IgM and IgA antibodies. Although this a promising diagnostic tool, the current sensitivity and specificity levels of this assay require improvement before it can be used clinically.

1.7 Immune Response to *Pneumocystis*

Once the fungus has entered the respiratory tract, antigen-presenting cells (APCs) can recognise components of the fungal cell wall or membrane. Such molecules include the MSG and β(1,3)-glucan, which are referred to as pathogen-associated molecular patterns (PAMPs) (Fig 2). The PAMPs are then recognised by pattern recognition receptors (PRRs), which include Toll-Like Receptors (TLRs) (2 and 4), and C-type Lectin receptors (CLRs) (Mincle, Dectin-1, Dectin-2). Pathogen recognition receptors are expressed on the surface of APCs, myeloid cells, and alveolar epithelial cells. Together the PAMPs and PRRs activate the APC to release cytokines, chemokines, and pro-inflammatory eicosanoids through the Nuclear factor Kappa B (NF-κB) pathway (Charpentier et al., 2021).

The interaction of CLRs and TLRs with β(1,3)-glucan on the cell wall of cysts results in the activation of the innate immune response, which in turn induces phagocytosis and the release of pro-inflammatory cytokines (Kutty et al., 2016). This is followed by the release of tumour necrosis factor α (TNF-α) through the translocation of NF-κB. Additionally, vitronectin and fibronectin, which are serum glycoproteins, bind to β(1,3)-glucan on the fungal cyst wall, thereby enhancing the alveolar macrophage (AM) response and resulting in increased production of interleukin (IL)-6 (Kelly and Shellito, 2010). The interaction between AMs and Dectin-1 is responsible for the non-opsonic phagocytosis of the fungus, which generates reactive oxygen species that are fungicidal (Steele et al., 2003).

Dectin-1 demonstrates elevated expression on AMs (Steele et al. (2003);Pop et al. (2006)). It recognises β-glucans on the cell wall of *Pneumocystis* and is responsible for the uptake and killing of the fungus, as well as producing pro-inflammatory mediators (Pop et al. (2006); Bello-Irizarry et al. (2012)). The dimerisation of Dectin-1 leads to the spleen tyrosine kinase (Syk) recruitment, which induces a signalling cascade through Caspase recruitment domain-containing protein 9 (CARD9). This signalling leads to the nuclear translocation of NF-κB, ultimately producing cytokines and chemokines to reduce the fungal pathogen (Skalski et al., 2015). Inhibition of Dectin-1 inhibits the non-opsonic phagocytosis and internalisation of *P. carinii* (Steele et al., 2003). Dectin-2 recognises the α-mannose structures on the surface of fungi and other microorganisms. Upon recognising the mannose structures, it couples with FcRγ to initiate downstream signalling that leads to the recruitment of Syk and CARD9 to activate the c-Rel subunit of NF-κB selectively (Sato et al., 2006). This signalling leads to the internalisation of the *Pneumocystis* and the release of cytokines such as IL-1β, IL-6 and TNF-α (Maldonado and Fitzgerald-Bocarsly, 2017).

Toll-like receptors expressed on AMs and dendritic cells (DCs) play a role in the inflammatory response against *Pneumocystis*. TLRs are classified according to the PAMPs they recognise (Kawai and Akira, 2007). Upon recognising different PAMPs, TLRs send a signal to the adaptor molecule myeloid differentiation factor 88 (MyD88) that signals downstream molecules belonging to the NF-κB and mitogen-activated protein kinase (MAPK) pathways (Bello-Irizarry et al., 2012). Ding et al. (2005) showed that *in vitro* and *in vivo* TLR4-deficient AMs had impaired CXCL1, IL-10, and IL-12p40 responses. Moreover, they observed that TLR4-deficient mice had elevated levels of TNF-α and IL-6 (Ding et al., 2005).TLR-2 knockout mice have shown decreased inflammatory responses against *P. murina,* and this decrease was correlated to increased disease severity (Wang et al., 2008).

Pneumocystis has a preferential adherence towards the alveoli of its host; thus, the AMs are the first line of defence in controlling the infection (Kelly and Shellito, 2010). The activation of AMs requires the presence of specific cytokines, including interferon-gamma (IFN-γ), TNF-α, and granulocyte-macrophage colony-stimulating factor (GM-CSF) (Martin and Pasula, 2000). Following the stimulation of these cells by IFN-γ, the macrophages can phagocytose and destroy both trophs and cysts. This phagocytosis can occur with or without opsonisation, with opsonisation occurring during the interaction of Dectin-1 and PAMPs (Steele et al., 2003). In response to phagocytosis, AMs produce a variety of pro-inflammatory cytokines, chemokines, and eicosanoid metabolites (Thomas Jr and Limper, 2004). While the mediators promote the clearance of *Pneumocystis*, they also promote pulmonary injury (Varela et al., 2011). Depletion studies of AMs have indicated a correlation between reduced AM levels and an increased incidence of severe pneumonia, as well as a diminished ability to clear pathogens. Rats that

have undergone depletion of AMs demonstrate an increased burden of *P. carinii* (Limper et al., 1997). Additionally, *in vitro* experiments revealed that AMs facilitated the binding, uptake, and killing of the fungus (Limper et al., 1997). *Pneumocystis* can subvert the functions of macrophages and cause them to undergo apoptosis, this is hypothesised to be a major host evasion strategy by the organism (Deckman et al., 2017). Macrophages are divided into classically activated macrophages (M1) and alternative macrophages (M2) subsets. While M1 macrophages are pro-inflammatory and play a major role in anti-fungal clearance, M2 macrophages are anti-inflammatory and are involved in tissue repair. The opposing effects between M1 and M2 macrophages are important in the immune response against *Pneumocystis*. Several studies have shown that M2 macrophages are the potent effectors cells against *P. murina* infection (Nelson et al. (2011); Nandakumar et al. (2017)).

Additionally, CD4+ and CD8+ T cells are activated, which then initiates an adaptive immune response (Kelly and Shellito, 2010). In the lungs, attachment of *Pneumocystis* results in diffuse alveolar damage. Moreover, the host's inflammatory response exacerbates lung damage, impeding gaseous exchange and resulting in diminished oxygen levels and potentially respiratory failure (Truong and Ashurst, 2023). In immunocompromised hosts with ineffective CD4+ cell responses, inflammatory cells accumulate and infiltrate the lungs which causes lung injury. CD4+ cells recruit and activate other immune effector cells such as AMs and monocytes to kill the organism. Hence people with low CD4+ cell counts (< 200 cells/mm^3) are more susceptible to PCP, this was particularly evident during the early years of the HIV/AIDS pandemic, where the prevalence of *Pneumocystis* was inversely proportional to CD4+ T cell count (Eddens and Kolls, 2015). It has also been shown in animal models that CD4-deficient mice are more susceptible to *P. murina*, while mice with severe combined immunodeficiency (SCID), characterised by the absence of functional T and B cells, tend to develop spontaneous PCP within 3 weeks (Gingerich et al., 2021). Reconstitution with CD4+ T cells from immunocompetent mice allows SCID mice to clear *P. murina* (Harmsen and Stankiewicz, 1990).T helper-type (Th) cells 1, 2, and 17 are a subset of CD4+ cells that are involved in the immune response against *Pneumocystis*. Th1 cells are activated by IL-12. In a previous study, Ruan et al. (2008) showed that the addition of IL-12 in CD4-deficient mice accelerated the clearance of *P. murina* along with elevated levels of TNF-α and IFN, while IL-12p35 deficient mice had delayed clearance of the infection. Similarly in humans, elevated levels of Th1 in the blood of PCP patients were associated with a better prognosis (Zhang et al., 2019). In contrast to a Th1 response, a Th2 response in *Pneumocystis* has been associated with an asthma-like pathology characterised by increased mucus production, airway narrowing, and tissue damage (Iturra et al., 2018). When both Th1 and Th2 responses are stimulated, there is an increase IFN-γ, TNF-α and Il-4 and IL-13 respectively (Shellito et al. (2000), Steele et al.

(2005); (Charpentier et al., 2021)). Th17 also has a pro-inflammatory response against *Pneumocystis*. Th17-deficient mice have been observed to have delayed *P. murina* clearance (Rudner et al., 2007).

CD8+ T cells are said to have a dual role in *Pneumocystis,* exhibiting immunomodulatory functions when present alongside CD4+ T cells and contributing to lung injury when CD4+ T cells are absent (Bhagwat et al., 2006). CD4+ T-cell-depleted mice have been shown to have a high influx of CD8+ cells. Despite this, mice still have a trend towards progressive PCP infection. Contrastingly, when both CD4+ and CD8+ cells are depleted, mice develop a more intense PCP infection (Beck et al., 1991). This suggests the importance of CD8+ cells in host defence against *Pneumocystis*. Kolls et al. (1999) showed that when they treated CD4+ T-cell-depleted mice with IFN-γ, there was increased clearance of *P. murina*. This resolution was associated with >4-fold increase in CD8+ T cells and natural killer (NK) cells, indicating that CD8+ T cells can clear *P. murina* in the absence of CD4+ T cells (Kolls et al., 1999).

B cells play a pivotal role in the immune response against PCP, exhibiting a dual function in antibody production and antigen presentation (Eddens and Kolls, 2015). Lund et al. (2006) showed that mice deficient in B cells have increased susceptibility to PCP compared to wild-type mice.

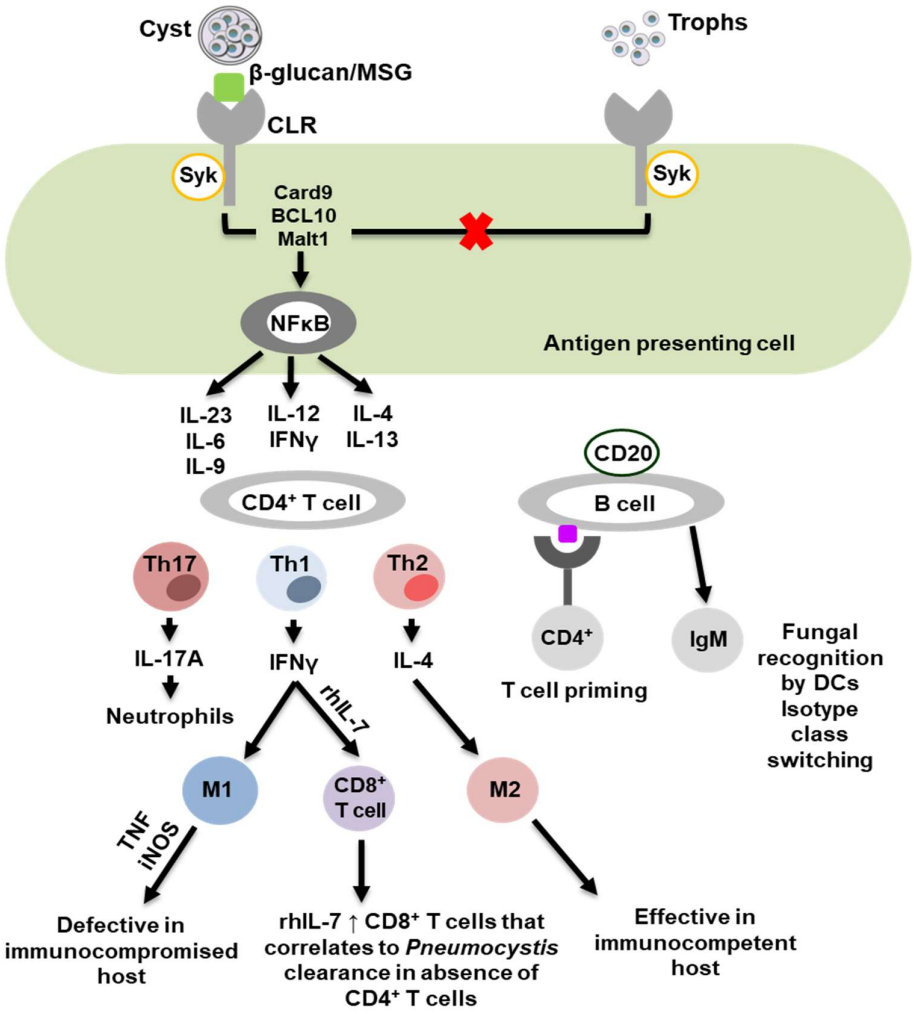

Figure 2 : The contribution of the host cell to the immune response against *Pneumocystis*

The *Pneumocystis* cysts and trophs through β(1,3)-glucan and MSG activate the immune response through NF-κB signalling that leads to activating a subset of CD4+ T cells and B cells. The subset of CD4+ T cells, Th1, Th2 and Th17, play an important role in *Pneumocystis* clearance. B cells are important in CD4+ T cell priming and antibody production (Otieno-Odhiambo et al., 2019)

2.0 *Pneumocystis* coinfection with viruses

Coinfections involve a variety of pathogens that can potentially have serious effects on the host. The presence of coinfection, while underreported, has the potential to influence the clinical progression, transmission, and control of infectious diseases. A systemic analysis by Griffiths et al. (2011) estimated that the prevalence of coinfections possibly exceeds one-sixth of the global population. A recent study of a paediatric population with respiratory infection reported coinfections in 23% of patients (McArdle et al., 2018). Viral and bacterial respiratory coinfections are well-established and are known for their severity through the subversion of

mucosal immunity, resulting in the inability to control bacterial replication (Bakaletz, 2017). Viral and fungal coinfections are an emerging area of interest that still require further investigations.

Viral and fungal coinfections are often associated with a worsened severity of outcomes to the host, and this is attributed to the fact that viruses damage the respiratory epithelium during infection and the dysregulation of immune cells, which allows fungi or other micro-organisms to attach and cause disease. This is demonstrated in studies involving influenza and *Aspergillus***,** SARS-CoV-2 and Mucormycosis, and SARS-CoV-2 and *Aspergillus* (Salazar et al., 2022). However, little is known about the effects that fungal pathogens have on the host that influence the outcome of viruses. The effects of coinfections do not always impact the health of its host negatively; the adverse effects can be antagonistic instead of additive or synergistic. Immune response against one pathogen can influence the immunity to a secondary unidentical pathogen, termed heterologous immunity (Agrawal, 2019). This response can result in an altered or enhanced immune response to a secondary pathogen due to a phenomenon known as "trained immunity" (Welsh et al., 2010). The result of this is influenced by multiple factors including; the virulent nature of the pathogens, the mode of infection, and the host's adaptive and innate immune responses (Salazar et al., 2022).

Respiratory syncytial virus (RSV) ranks among the most prevalent infectious pathogens linked to pneumonia in paediatric populations. Natural infection with viruses such as RSV does not confer protection, and subsequent infections throughout life are usually more severe, and this is attributed to the induction of a powerful cellular immune response. This was particularly evident with the administration of formalin-inactivated RSV in children during the 1960s which led to enhanced respiratory diseases and high hospitalisations (Ruckwardt et al., 2019). Given the challenges in developing suitable vaccine candidates, studies have sought out mechanisms to modulate the host immune response to subsequent infections instead of developing novel vaccines (Williams et al., 2004). *Pneumocystis murina* has been shown to protect mice against subsequent influenza infection (Wiley and Harmsen, 2008). Thus, previous *P. jirovecii* exposure can affect RSV.

2.1 Epidemiology, Diagnosis and Management of RSV

RSV is a common infection during infancy, often leading to pneumonia or severe lower respiratory tract infection (LRTI). RSV is the leading cause of paediatric respiratory illness in children <5, with common re-infections throughout life (Salimi et al., 2021). It is estimated by WHO that a third of the annual deaths in children <5 are a result of acute LRTI (Simoes, 1999). Current annual estimates of the global impact reveal that RSV is responsible for 3 million hospitalizations and 60 000 in-hospital deaths in children (Shi et al., 2017). In developing

countries, RSV has mortality rates ranging between 55,000 and 200,000 annually in children. This was evident in the Drakenstein study in which the majority of the pneumonia cases in children were due to a viral infection (Zar et al., 2016). Furthermore, RSV contributes substantially to hospitalisation among the elderly.

Children <6 months of age have more pronounced morbidity and mortality, with more than 50% hospital deaths. Low- and middle-income countries contribute more to the global incidence of RSV (Zar et al., 2016). RSV is likely underreported due to a lack of routine testing, particularly in poor resource settings. The lack of therapeutic agents against the disease further contributes to disease severity and incidence, resulting in substantial healthcare costs and burdening the economy. Despite its severity and mortality, RSV has no curative therapeutic available, current methods are aimed at prevention.

RSV symptoms in the upper respiratory tract include rhinitis, fever, cough, and acute otitis media, while lower respiratory tract symptoms can involve dyspnoea and chest wall in-drawing (Simoes, 1999). Infants may show nonspecific signs like poor feeding and lethargy, with severe cases leading to respiratory failure. In adults, symptoms range from mild cold-like symptoms to severe distress. Diagnosis involves PCR testing and virus culture. As of 2023, Nirsevimab, a long-lasting monoclonal antibody, is licensed for infant immunisation (Griffin et al., 2020). Severe RSV management focuses on supportive care, with Ribavirin used for infants with bronchiolitis and immunocompromised patients.

2.2 Biology of RSV

RSV is a member of the *Pneumoviridae s*ubfamily, an enveloped negative-strand virus with a single-stranded RNA genome. The human RSV (hRSV) pathogen is closely related to other species of RSV, including bovine RSV (bRSV), ovine RSV (oRSV), and mice RSV (PVM) (Bem et al., 2011). The single-stranded RNA virus consists of 11 proteins, of which only two allow attachment to the respiratory epithelium (Kaler et al., 2023). This virus has a helical nucleoplasm with a diameter between 150nm and 200nm. RSV has a non-segmented but mutable genome. The RSV genome codes for 8 structural proteins and two unique non-structural proteins, namely, NS1 and NS2. There are two subgroups, RSVA and RSVB based on their antigenic variability.

The three proteins that comprise its envelope are the attachment protein (G), the Fusion protein (F), and the SH protein. The G and F proteins are of significant importance in the pathogenesis of RSV and are additionally regarded as the primary antigenic determinants. The G protein enables attachment to the host, while the F protein functions in cell entry and fusion (Battles and McLellan, 2019). The exact function of the SH protein is unknown, but

recently it has been shown to have antiapoptotic properties. The other structural proteins include the large protein, nucleocapsid, matrix, non-structural proteins 1 and 2, and the phosphoprotein (Borchers et al., 2013).

2.3 Pathogenesis of RSV

Infection with RSV occurs when the aerosolised particle is inhaled or through contact with the virion in the environment. RSV travels from the upper respiratory tract and eyes, to incubate for 3-8 days, with symptoms appearing by day 5 (Collins and Graham, 2008). In the initial stages of infection, there is robust replication of RSV in the nasopharynx, reaching titres of approximately 10^6 plaque-forming units (pfu) (Domachowske and Rosenberg, 1999). RSV infects the ciliated epithelial cells of the upper and lower respiratory tract, Type 1 pneumocytes, as well as intraepithelial cells (Schmidt and Varga, 2017) . The airway epithelium serves as the primary site for viral replication.

Upon entry into the host, the G and F glycoproteins mediate attachment into the respiratory epithelium. The epithelial cells then proceed to alert the immune system to inhibit viral replication and spread, and to clear the infection. However, RSV's evolution in evading recognition allows it to replicate within viral inclusion bodies in the cytoplasm of epithelial cells (Parsons et al., 2024). These viral inclusion bodies are said to be viral factories where viral RNA synthesis occurs (Galloux et al., 2020).Subsequently, the bronchial epithelial cells become infected, this is the site where viral replication is the most effective, resulting in the inflammation of the peribronchiolar region (Simoes, 1999). Peribronchial monocytes and T cells infiltrate causing epithelial necrosis, submucosal oedema, and mucus overproduction (Jha et al., 2016). The epithelium slows off, obstructing the small airways, and mucus plugs.

In the mouse model of hRSV infection, a high intratracheal (IT) inoculum is administered to detect LRTI since RSV is not a natural murine pathogen (Hennus et al. (2012) ; (Borchers et al., 2013)). The symptoms and signs usually include weight loss, ruffled fur, reduced activity, and lethargy. Mice deficient in TLRs (2,4,6,7) have shown increased susceptibility to hRSV (Bem et al., 2011). Most knowledge of the pathogenesis of RSV is from animal models, particularly the inbred mice strains which are also semi-permissive to the hRSV. In these animal models, acute RSV can result in airway obstruction. Macrophages have been identified as the main contributors of CCl3, CCL5, TNF-α, IFN-γ, and IL-6 production. In depletion studies of macrophages, it was observed that their inhibition results in inactivation and non-recruitment of NKs, with CD4+ and CD8+ T cells unaffected (Pribul et al. (2008); Borchers et al. (2013)). The observed histopathological alterations in mice inoculated with high doses of

hRSV include perivascular and peribronchial macrophage, lymphocyte infiltration, interstitial pneumonia, and scattered neutrophils (Bem et al., 2011).

Pneumonia virus of mice (PVM), a murine homolog of RSV, replicates in the lower respiratory tract, with peak titres of 10^8 pfu (Domachowske et al., 2000). Mice infected with PVM show symptoms of severe disease, with significant weight loss, and mortalities of up to 100% (Domachowske et al., 2002). Histopathology of PVM-infected mice reveals neutrophilic infiltration which propagates to alveolitis and alveolar oedema (Garvey et al., 2005). There is also apoptosis of the alveolar epithelium, profound inflammation and severe pulmonary oedema, as well as recruitment of granulocytes (Dyer et al., 2012). The most prevalent cytokines are TNF-α, IL-6, murine MIP-2 and murine keratinocyte-derived protein chemokine KC, RANTES, IFN-γ, CCL3, as well as CCL2 (Bem et al., 2011).

2.4 Immune response to RSV

As alveolar epithelial cells (AECs) are the primary site of RSV infection, upon infection they induce the production and recruitment of chemoattractant and adhesion molecules that subsequently trigger the innate and adaptive immune systems (Agac et al., 2023). Several elements of the innate immune system contribute to the control of RSV infection. These include epithelial cells, DCs, macrophages, monocytes, granulocytes, various PRRs, cytokines, chemokines, cellular stress, and apoptosis. The initial innate immune detectors of RSV are PRRs. RSV can be detected by three classes of PRRs, namely, TLRS, retinoic inducible receptors (RLRs), and nucleotide binding-oligomerisation domain (NOD) like receptors (NLRS) (Zeng et al., 2012). Upon recognition of specific PAMPs on RSV, adapter molecules, including MYD88, TIR, TRIF, and TRAM, are recruited, which subsequently activate the transcription factor NF-κB, pro-inflammatory genes such as TNF-α, IL-1β, and IL-6, which are TRIF-dependent, and interferon regulatory factors (IRFs), which regulate the expression of pro-inflammatory cytokines and type I and III interferons (I IFN & III IFN) (Sun and López, 2017).

TLRs expressed either on the plasma membrane or intracellularly interact with RSV, and their interaction leads to the recruitment of Toll/IL-1 receptor (TIR), which contains MyD88 and TRIF. Furthermore, NF-κB, IRFs and MAPK are activated to control the expression of cytokines, chemokines and IFN-I (Parsons et al., 2024).TLR4 was the first receptor identified to play a role in the clearance of RSV and has thus been studied extensively. TLR4 recognises LPS on the surface of gram-negative bacteria and mediates a signal through TRIF, or MyD88 pathways, and in the case of RSV, TLR4 recognises the F protein to activate an innate immune response (Stephens and Varga, 2020). Studies with TLR4-deficient mice have shown delayed

viral clearance, reduced NK and CD14+ cell recruitment, and impaired NK cell function (Haynes et al., 2001). This indicates that a shared receptor activation pathway can be induced in bacterial, fungal, or other viral infections (Churiso et al., 2022). Polymorphism studies of TLR4 have shown that mutations in the receptor are associated with severe RSV bronchiolitis (Caballero et al., 2015). Other TLRs that play a role in RSV are TLRs 2, 3, 6 and 7. TLR2 is located on the cell surface to recognise cell wall components such as lipoprotein and peptidoglycan (Kim and Lee, 2014). Upon recognition of the cell wall compartment, there is innate immune activation via the MyD88-mediated pathway. In deficient studies of TLR2, there are reduced pro-inflammatory cytokines, impaired neutrophil migration into the lungs, and uncontrolled virus replication (Murawski et al., 2009). TLR2 and 6 deficient mice have impaired early production of IL-6 and type I IFNs (Murawski et al., 2009). The deficiency of TLR3 and 7 skews the inflammatory environment in the lung, leading to increased mucus production and worsened lung epithelial hyperplasia, with viral clearance unaffected (Rudd et al. (2006); Sun and López (2017)).

Type I interferons are antiviral cytokines that activate their receptors in an autocrine or paracrine manner to activate the JAK/STAT-mediated signalling cascade, leading to the expression of interferon-stimulated genes (ISGs) that interfere with viral replication and the pro-inflammatory response, thus contributing to viral clearance. IFN-α or IFN-β mediate early viral control through the IFN receptor (IFNAR) to produce ISGs. Their signalling modulates metabolic pathways that set the AECs in an antiviral state to restrict viral replication and spread (Agac et al., 2023). Type I IFNs also result in the production of pro-inflammatory cytokines such as IL-6, TNF, and IFN-γ (Stephens and Varga, 2020). Infants infected with RSV have been shown to have high concentrations of type I IFNs in the alveolar and bronchial epithelial cells infected (Reed et al., 2009). IFNAR-deficient mice exhibited increased viral burden, weight loss and reduced pro-inflammatory cytokines following RSV challenge compared to WT controls (Goritzka et al., 2014). Type I IFNs also induce the maturation of DCs, T cell differentiation and establishment of T cell memory, and enhance NK response (McNab et al., 2015).

Various elements of the adaptive immune response contribute to RSV clearance. These include CD4+ and C8+ T cells and antibodies. Dendritic cells link the innate immune response to the adaptive immune system by priming T and B cells to encounter antigens through their major histocompatibility complex (MHC) receptor-, T cell receptor- (TCR) and B cell receptor (BCR) interactions and the secreted cytokines. Infection with RSV results in the recruitment of CD4+ cells to the airway to orchestrate an immune response by secreting IL-17, IFN-γ, and TNF-α (Agac et al., 2023). Infants with severe RSV have been shown to have a reduced number of CD4+ T cells and TNF-α compared to infants with less severe symptoms. The

release of pro-inflammatory cytokines by CD4+ T cells is important in regulating the innate and adaptive immune response clearing the virus. However, exacerbated pro-inflammatory response and thus an imbalanced TNF-α may lead to a worsened disease severity. A dysfunctional CD4+ T cell response can lead to a Th2 immune response indicated by the cytokines IL-5 and IL-13. This response leads to increased mucus secretion and airway hyperresponsiveness as shown in the study by Waris et al. (1996) in which mice were infected with formalin-inactivated RSV. Formalin-inactivated RSV was previously a vaccine candidate that caused excessive RSV disease in infants upon subsequent RSV infection.

CD8+ cells kill the virus through their cytotoxic activity by inducing apoptosis of the target cells and secreting perforins and granzymes (Schmidt and Varga, 2018). Furthermore, they secrete cytokines such as IL-2, IL-10, IFN-γ and TNF-α. CD8-deficient mice have been shown to have delayed RSV clearance compared to uninfected mice, while adoptive transfer of these CD8+ cells led to reduced viral burden and weight loss, and increased IFN-γ (Kinnear et al., 2018). This is further supported in human studies in which reduced CD8+ cell counts in the blood of RSV-infected individuals were associated with delayed viral clearance and worsened disease severity (Welliver et al., 2007). CD8+ T cells have also been shown to suppress the Th2 immune response, thus regulating the CD4+ response. Despite their antiviral properties, CD8+ cells are involved in the pathology following RSV infection. This is evident in mice when CD8+ T cells were passively transferred to RSV-infected mice, and the result was increased virus clearance with enhanced lung pathology (Cannon et al., 1988).

The antibody response during RSV infection targets the F and G proteins (Russell et al., 2017). When the virus enters the body, B cells secrete virus-specific antibodies that neutralise the virus and block the binding domain of the virus (Agac et al., 2023). Survival markers of B cells, such as B cell-activating factor (BAFF) and A proliferation-inducing ligand (APRIL), are upregulated in mice infected with RSV (McNamara et al., 2013). While B-cell stimulating factors are in high concentrations, the levels of T-cell-dependent cytokines are low.

2.5 Summary

Resource-limited countries, particularly in sub-Saharan Africa, face significant challenges when treating patients with HIV-associated *Pneumocystis jirovecii* pneumonia, as discussed above. Furthermore, considering the high prevalence of coinfection in these patients and healthy individuals, data on the host immune response during these interactions is scarce. Therefore, in the completion of this MSc project and as part of a larger research programme funded through the National Institute for Health and Care Research (NIHR-UK), we identified Kex1 as a promising tool in developing an immunodiagnostic assay against *Pneumocystis.*

We show that Kex1 recognises *P. murina*-infected mouse samples, including lung tissue, urine and serum and will support the development of a potential rapid diagnostic for PCP. Furthermore, to evaluate the effect of *Pneumocystis* exposure on the disease outcome of a common viral pathogen, RSV, we used our established mouse model of disease to scrutinise the host immune responses. Our data demonstrates that the immune responses triggered by *Pneumocystis* reduce the viral load and associated host responses, potentially providing protection from severe pneumonia. Next, we will identify the mechanism behind this protection and whether *Pneumocystis* can reduce the pathology during RSV pneumonia and evaluate whether these responses can indeed protect mice.

3. Methods and Materials

3.1 Mice

Eight- to twelve-week-old C57BL/6 and RAG1-deficient mice were used in this study. These mice were housed in specific pathogen-free conditions of the animal unit at the University of Cape Town (UCT), faculty of Health Sciences, Animal ethics committee (FHS AEC REF NO: 023_007).

3.2 *Pneumocystis murina* propagation

To generate new infected lung stocks, RAG-1 -/- mice were infected with *P. murina* from lung suspension of previously infected mice. The mice were then monitored for 5-8 weeks. Once the mice had reached the 20% body weight loss, they were euthanised, and the were lungs collected and stored in PBS at -80 °C. Serum and urine samples for evaluation of the Kex1 antiserum were also collected at this point and stored at -80 °C.

3.3 Preparation of *P. murina* inoculum and infection

For the preparation of the inoculum, a thawed lung from an infected mouse was processed by mashing it through a 70 µm cell strainer in 4 ml of phosphate-buffered saline (PBS). Subsequently, a 1/10 dilution of this sample was prepared, and 5 µl was spread evenly in each of the 10 mm diameter circles on Fisherbrand™ Fluorescent Antibody Microscope Slides (Catalog No.22-339408) for cyst counting. After the slide was air-dried, it was stained using Diff-Quick (Difco, Detroit, MI) staining solution. Cysts were then counted under a light microscope at 100x magnification, and their concentration was calculated using the formula: πr^2 where r = number of cysts counted across the diameter of the circle/2. The lung suspension was then diluted with the required volume of PBS to achieve 2×10^6 cysts/ml.

To infect the mice, a final concentration of 2×10^5 cysts in 100 µl was administered via the intratracheal (IT) route. On the day of the procedure, both the *P. murina*-only group and the coinfected group of mice were anaesthetised using a combination of ketamine and xylazine (80mg/kg and 16mg/kg respectively) i.p injection. Following anaesthesia, the mice were suspended vertically by their incisors on a suture wire. The tongue of each mouse was then extended to the left to facilitate access to the trachea, through which 100 µl of the inoculum was instilled intratracheally using a pipette. The mice were monitored daily after infection until they reached the predetermined endpoints.

3.4 RSV Stock propagation and infection

To make RSV stocks for infection, Hep-2 cells were grown in tissue culture flasks in Dulbecco's modified Eagles's medium (DMEM) containing 10% foetal bovine serum (FBS). Cells were infected with RSV(A2) when they were 70% confluent. The final virus concentration was 0.1 pfu/cells. The virus was allowed to adsorb to cells in serum-free medium for 1 hour. The infection was carried out at 37°C in a 5% CO_2 atmosphere. FBS was added after adsorption, and the flasks were incubated for 2-3 days. To collect the virus, the supernatant along with RSV-infected cells were harvested. The infected cells in the culture medium were sonicated at 4°C on ice. The virus in the supernatant stocks were collected and aliquoted as virus stocks after centrifugation at 3000 rpm for 10 min at 4°C to remove cell debris. The stocks were snap-frozen in liquid nitrogen and then stored at -80°C until required. A plaque assay was done to assess the stock virus concentration. The groups infected solely with RSV and those with co-infections were anaesthetised as above and received an intranasal instillation of 50µl of the stock solution.

3.5 *P. murina* and RSV Inoculation

In the coinfection mouse model, mice were subjected to infections with *P. murina* and RSV, utilising different doses of RSV and varying experimental timelines. Each experiment comprised three groups of mice: a control group infected solely with *P. murina*, a control group infected solely with RSV, and a group coinfected with both *P. murina* and RSV. For all experiments, *P. murina* was administered via intratracheal instillation of 100 µl containing 2×10^5 cysts while the mice were under anaesthesia. In the first experiment, wild-type (WT) mice were infected with *P. murina* for 14 days. On the 14th day, these mice were coinfected with 2.5×10^5 PFU of RSV for an additional 7 days, after which they were euthanised on day 21 post *P. murina* infection. In experiment 2, WT mice were infected with *P. murina* for 7 days, followed by coinfection with 5×10^5 PFU of RSV for another 7 days, and euthanasia on day 14 of *P. murina* infection. In experiments 3 and 4, WT and RAG mice, respectively, were infected with *P. murina* for 7 days, followed by RSV infection for 4 days, and subsequently euthanised on the 4th day of RSV infection, which corresponds to the peak of viral replication.

3.6 Mice euthanasia and sample collection

Mice were euthanised with slow rising halothane (5% in air). Following euthanasia, cardiac puncture was performed to obtain blood samples, which were collected in BD Microtainer® blood collection tubes for separation of serum from the blood clot. Serum samples were obtained by centrifugation of blood collection tubes (4 °C, 10,000 *xg* for 10 min) which were

stored at -80 °C for future analysis. The lungs were excised under aseptic conditions, and the various lobes were allocated to distinct, labelled tubes. The left lung lobes were preserved in 10% formalin for histological analysis, while the middle and inferior lobes were kept in phosphate-buffered saline (PBS) supplemented with a protease inhibitor for the assessment of tissue cytokines. The superior lobes were stored in Trizol for subsequent PCR analysis, and the variable middle lobe was stored for plaque assays. All samples were subsequently stored at -80°C until further analysis.

3.7 Plaque Assay

To assess the RSV concentration, Hep-2-cells were transferred into a 96-well plate in DMEM + 10%FBS and incubated at 37°C until 70% confluent. Virus stocks or lung samples from RSV-infected mice that were previously stored at -80 °C were homogenized in serum-free DMEM (sfDMEM) to generate a virus suspension. Media from the confluent Hep-2 cells was expelled, and 50 µl virus suspension (or respective dilution) was added to each well. For a positive control, 50 µl of thawed RSV stock (or respective dilution) was used. The plates were incubated for 2 h at 37°C, after which 150µl/well of DMEM + 10% FBS was added, followed by a further 18 h incubation. Media was expelled, and cells were washed with PBS and fixed with 100µl/well of absolute methanol for 20 minutes. Cells were then washed with 200µl/well of PBS/1%BSA and blocked with the same solution for 1 hour. One hundred microlitres per well of biotin anti-RSV antibody (1/150) (AB19986, Abcam) was added to incubate for an hour at room temperature. This was followed by washing with 200µl/well of PBS/1%BSA twice, and then the addition of ExtrAvidin peroxidase (E2886, Sigma-Aldrich) (1/500) for 30 minutes. Plates were then washed, and 50µl/well of SIGMAFAST™ DAB substrate (Sigma-Aldrich, D0426) was added until the plaques had acquired the desired colouration. To stop the reaction, the wells were washed with PBS. Finally, plaques were counted using a dissection microscope and no. pfu/ml were calculated.

3.8 RNA isolation, cDNA synthesis and quantitative qPCR

Total RNA was isolated from lung tissue of the infected mice using Trizol (Life Technologies) method as per the manufacturer's instructions. Equal amounts of RNA (1 µg) for each sample were used for cDNA synthesis using RevertAid RT Reverse Transcription Kit (Thermofisher Scientific, K1691), then *P. murina* burden was quantified using SsoAdvanced quantitative qPCR Universal Probes Supermix (Bio-Rad, 1725281) with the following *P. murina-specific* mtSSU rRNA primers and probe.

Forward: CATTCCGAGAACGAACGCAATCCT

Reverse: TCGGACTTGGATCTTTGCTTCCCA.

FAM probe: TCATGACCCTTATGGAGTGGGCTACA

A standard curve of 10^8 to 10^0 mtSSU copies was prepared using previously generated arbitrary cDNA standard.

Following cDNA synthesis, quantification of viral copies was performed for the RSV L gene using the following primers:

Forward (300 nM): GAACTCAGTGTAGGTAGAATGTTTGCA

Reverse (300 nM): TTCAGCTATCATTTTCTCTGCCAAT.

FAM probe (175 nM): TTTGAACCTG TCTGAACATTCCCGGTT

A standard curve of 10^8 to 10^0 L gene copies was prepared using previously generated arbitrary cDNA standard.

qPCR was performed using using a LightCycler® 480 instrument (Roche). PCR cycling conditions were as follows: one initial denaturation step at 95°C for 30s, followed by 50 cycles of (95°C for 5s, 60°C for 10s [acquisition step] and 72°C for 1s).

3.9 Relative quantification of Interferon-β transcript levels

Quantitative PCR was performed on cDNA samples to quantify the relative levels of interferon-β transcript levels between groups. qPCR was done using LightCycler® 480 SYBR Green I Master mix (Roche, 04707516001). The levels of IFN-β were normalised to the levels of a reference gene, GADPH. The following primers were used at 300 nM final concentrations:

GADPH

Forward: CATCACTGCCACCCAGAAGACTG

Reverse: ATGCCAGTGAGCTTCCCGTTCAG

IFN-β

Forward: GCCTTTGCCATCCAAGAGATGC

Reverse: ACACTGTCTGCTGGTGGAGTTC

3.10 BCA Assay

To quantify the total protein concentration of samples for normalisation, lung supernatants were diluted in PBS. A BCA assay was performed in a 96-well plate using a Pierce™ BCA Protein Assay Kit (23227, ThermoFisher Scientific) as per the manufacturer's instructions. The absorbance was measured on the VERSA max Tunable Microplate Reader (Molecular Devices Corporation, California, US).

3.11 Tissue cytokine profile

The supernatant obtained from lung tissue was utilized to assess the levels of cytokines. The cytokine profiles in the tissues were evaluated using the OptIEA kits for mouse TNFα, IFN-γ, IL-6, IL12-p40, and IL12-p70 (BD Biosciences), or mouse IL-1β DuoSet ELISA kit (DY401, R&D Systems), following the manufacturer's guidelines. Briefly, 96-well plates were coated with 100µl of capture antibody and incubated overnight at 4°C. The following day, the plates were washed with wash buffer (0.05% Tween 20 in PBS). This was followed by a blocking step, where 200µl of blocking buffer was added per well and allowed to incubate for one hour at room temperature. During this blocking period, standards and samples were diluted according to the manufacturer's instructions. After the incubation, the plates were washed 3 times. Diluted standards and samples were then added to the plates, which were covered with an adhesive strip and incubated for 2 hours at room temperature. Following this incubation, the plates were washed 5 times, or 3 times for the IL-1β assay. For the IL-1β plate, 100µl of detection antibody diluted in reagent diluent was added and incubated for an additional 2 hours. For the other cytokines, 100µl of the working solution (detector + Streptavidin-HRP) was introduced into the wells and incubated for an hour. The plates were then washed 7 times and developed using tetramethylbenzidine (TMB) substrate at a volume of 100µl/well. After the two-hour incubation with the IL-1β detection antibody, the plate was washed 3 times, and 100 µl of working dilution of streptavidin-HRP was added, followed by a 20-minute incubation. The plate was washed again, and 100µl of substrate solution was added to each well for 20 minutes at room temperature. To stop the reaction, 50µl/well of 2N sulfuric acid was added, and the absorbance was measured at 450 nm, with 570 nm wavelength correction, within 30 minutes of stopping the reaction using a VERSA Max Tunable Microplate Reader (Molecular Devices Corporation, California, US). Cytokine data are expressed as pg cytokine per mg of total protein.

3.12 Serum Antibody ELISA

The total levels of IgG, IgG1, IgM, Ig2a and Ig2b antibodies in the serum of the three groups were quantified using antibodies and standards purchased from Southern Biotech (Birmingham, AL). Coating of the Nunc-Immuno Maxisorb 96-well plates with goat-anti-mouse capture antibody at a dilution of 1:1000 was conducted at 4°C overnight. Subsequently, the plates were washed on the following day with a wash buffer (0.05% Tween 20 in PBS) three times. Following this, the plates were blocked with 2% BSA in PBS for two hours at 37°C. The plates were then washed four times, and the diluted serum samples (1:1000 in 1 × PBS) were added. The plates were incubated overnight at 4°C. The plates were washed four times the following day and the diluted alkaline phosphatase rat anti-mouse secondary antibody (1:2000) was added. The plates were then incubated for three hours at 37°C. To develop the plates, 50 µl per well of 1 mg/ml 4-nitrophenyl phosphate disodium salt hexahydrate substrate solution (Sigma-Aldrich, UK) was added and left to develop in the dark. The absorbance was then measured after 20 mins on the VERSA Max Tunable Microplate Reader (Molecular Devices Corporation, California, US).

3.13 Kex1 Western Blot and Indirect ELISA

Prof. Chris Thornton (University of Exeter) has used a synthetic antigen derived from Kex1, a protease specific to *Pneumocystis,* to generate antiserum in rabbits. The Kex1 epitope is conserved across *Pneumocystis* species. We used this antiserum to attempt detection of PCP in protein samples from *Pneumocystis*-infected mice, using Western blot and ELISA. Infected samples were obtained from mice previously used in *P. murina* propagation at the humane endpoint (20% weight loss) and stored at -80 °C as described in Methods in Materials. Lung extracts were prepared by mashing thawed whole lungs through a 70 µm filter and resuspending in 4ml of PBS with protease inhibitor. Dot blots were performed by spotting 10 µl of protein sample on prepared PVDF membrane and allowing to air-dry before proceeding with the blocking step. Protein samples for SDS-PAGE were prepared by adding an equal volume of 2x Laemmli sample buffer and incubation at 95°C for 10 min. Protein samples were then centrifuged and the supernatant was collected. Equal amounts of 10µl of the sample were added to the lanes. They were then separated on a 12% SDS-PAGE gel and then transferred to a PVDF membrane (which had been prepared by soaking the membrane in methanol for 5 min, followed by rinsing with distilled water). After blocking with 5% BSA in PBS, the membranes were washed 3 times with 1% BSA in PBS and then probed with 1/20,000 of the primary antibody (Kex1 antiserum) for 24 hours. The membranes were then washed with shaking for 5 minutes. This was repeated 3 times. The membrane was then probed with a secondary antibody solution Alkaline Phosphatase-Conjugated (Anti-Rabbit) (Thermofisher

Scientific, WP20007) for an hour while shaking. This was followed by another wash step (5 washes with 50 mM Tris-HCl pH 8), after which a Novex® AP chromogenic substrate (Thermofisher Scientific) was added and incubated until the desired band intensity was achieved. The reaction was then stopped by rinsing the blot briefly with water. The membrane was allowed to air-dry and was then photographed.

Detection of Kex1 using an indirect ELISA was attempted. Lung homogenate samples were diluted 1:3 with bicarbonate buffer pH9.0 and 100 µl diluted sample was added to ELISA plates and incubated overnight at 4°C. The following day, the plates were washed five times with 0.05% Tween-20 in PBS, then blocked with 1% BSA in PBS for 1 hour. One hundred microlitres per well of anti-rabbit secondary antibody conjugated to biotin (1:40,000) (Abcam, AB6720) was added for 2 hours at room temperature, followed by 3 washes. Streptavidin–HRP (Thermofisher Scientific, 434323) was added for 30 minutes, followed by 5 washes. The plates were then developed using TMB substrate followed by measurement of absorbance as described above for tissue cytokine ELISA.

3.14 Histology

The left lung lobes were harvested and subsequently fixed in a 10% formalin solution prior to the processes of embedding and sectioning. Staining procedures used were Grocott's methenamine silver stain (GMS), haematoxylin and eosin (H&E), and periodic acid-Schiff (PAS). The lungs were embedded in wax and trimmed into thin sections which were allowed to flow in a warm water bath. The sections were then placed onto glass slides and incubated at 37°C for 2-18 hours to remove the wax. The tissue was then rehydrated. Following the rehydration, the tissues underwent GMS staining to identify fungal organisms, H&E staining to visualize inflammatory cells, and PAS staining to assess mucus production. A certified technician performed the processes of dehydration, sectioning, and staining. Photomicrographs of the stained sections were captured using a Zeiss Axioskop M upright microscope with a colour AxioCam HRc camera.

3.15 Statistical analysis

Statistical analysis was performed using Graph Pad Prism version 6.01. The values were reported as the mean ± SEM or SD unless indicated otherwise. Differences across groups were analysed using multiple t-tests or one-way ANOVA using the Brown–Forsythe test as stated. Differences between two groups were analysed using unpaired t-tailed student tests with statistical significance represented as *: p=0.05, **p=0.01, ***p=0.001, ****p<0,0001

3.16 Ethics

This work is part of a study approved by the UCT Animal Ethics Committee (protocol number 023-007). All work is performed within the confines of the procedures and experimental design of the protocol as authorised or as amended.

5. Results

5.1 Detection of Kex-1 in RAG-1 -/- mice experimentally infected with *P. murina*

This study aims to evaluate polyclonal antiserum (pAb) raised against a *Pneumocystis* biomarker, Kex1, to develop a lateral-flow assay (LFA) for rapid point-of-care diagnosis of PCP. This biomarker is conserved across *Pneumocystis* species, allowing the Kex1 antiserum to be tested against *P. murina* from infected mice before the final application in the diagnosis of *P. jirovecii* infection in patients. The antiserum was developed by Prof. Thornton (University of Exeter) in which rabbits were inoculated with a synthetic Kex1 antigen, followed by antiserum collection and purification after 60 days. Using this antiserum, proof-of-principle experiments investigated the detection of the biomarker in lung, urine and serum from *P. murina*-infected RAG-1-/- mice, using immunoblotting (as described in Material and Methods)... Infected mice were euthanised at 20% weight loss (8-12 weeks) and samples were collected, processed and stored at -80 °C. Samples from naïve (uninfected) RAG-1-/- mice were collected and stored as negative controls. Samples were analysed by dot blot (Fig 3 A, B, and C), SDS-PAGE and Western blot using anti-Kex1 diluted to 1/20,000. Kex1 was detected in lung homogenates, urine and serum from infected mice through a dot blot. The lung homogenates were further tested using SDS-PAGE and Western blot. A protein approximately 100 kDa in size was detected, while smaller bands thought to be degradation products of approximately 63 kDa were observed. Similarly, Kex1 bands were also visible in serum (Fig 4B) and non-specific binding in naïve samples was minimal.

In contrast to the Western blot results, the attempted detection of Kex1 using indirect ELISA resulted in higher absorbance values for naïve samples compared to infected samples. This may indicate non-specific binding of Kex1 or the secondary antibody, or an unanticipated binding of the streptavidin-HRP to endogenous biotin present in the samples (Fig 5A).

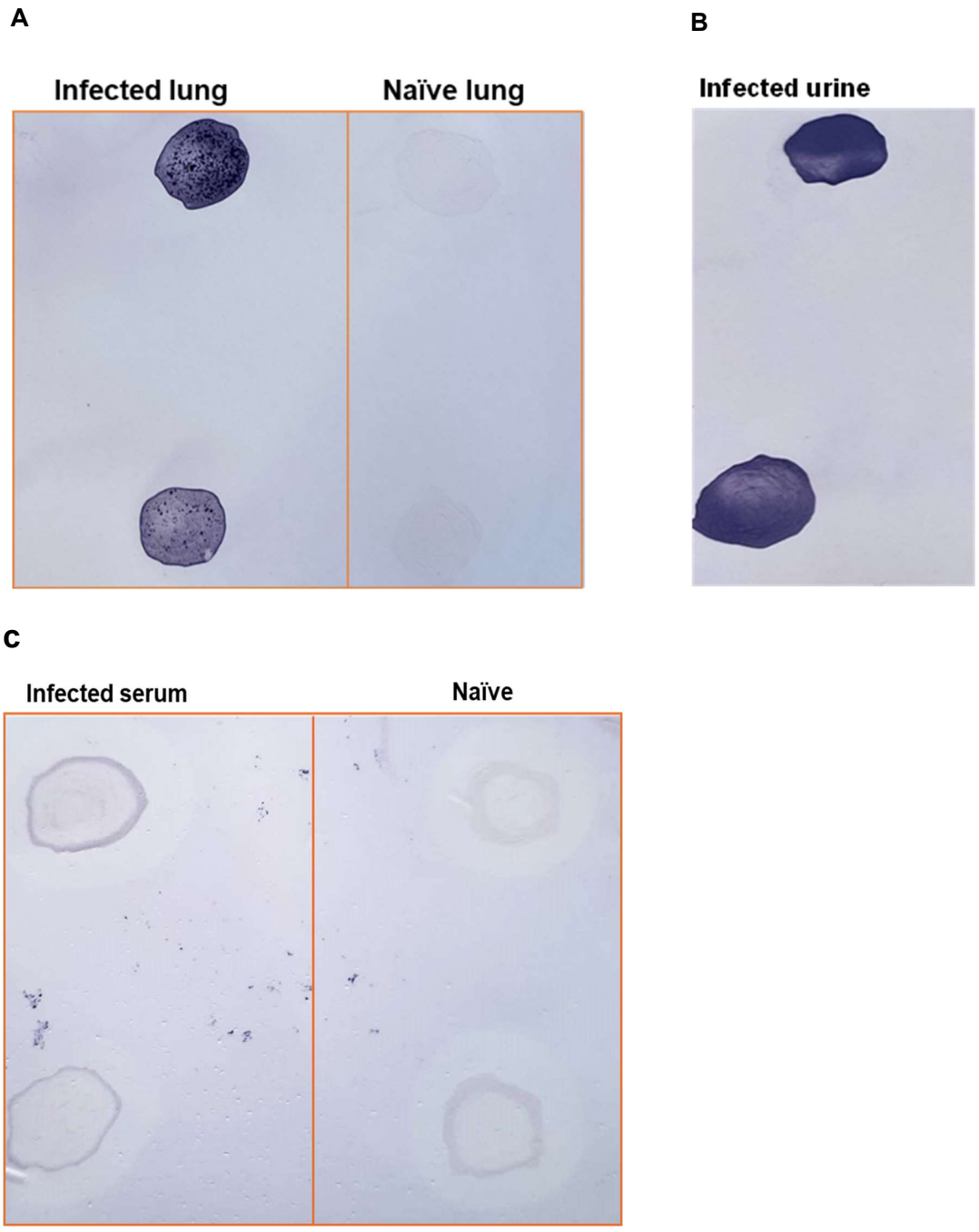

Figure 3 : Dot blot detection of *P. murina* Kex1.

RAG-1-/- mice were infected with *P. murina.* and samples were collected: lung homogenates (A), urine (B) and serum (C). Control samples were collected from uninfected (naïve) RAG-1-/- mice of the same age. Using a polyclonal antiserum raised in rabbits against Kex1. A protein was detected in the infected samples with minimal binding on the naïve samples.

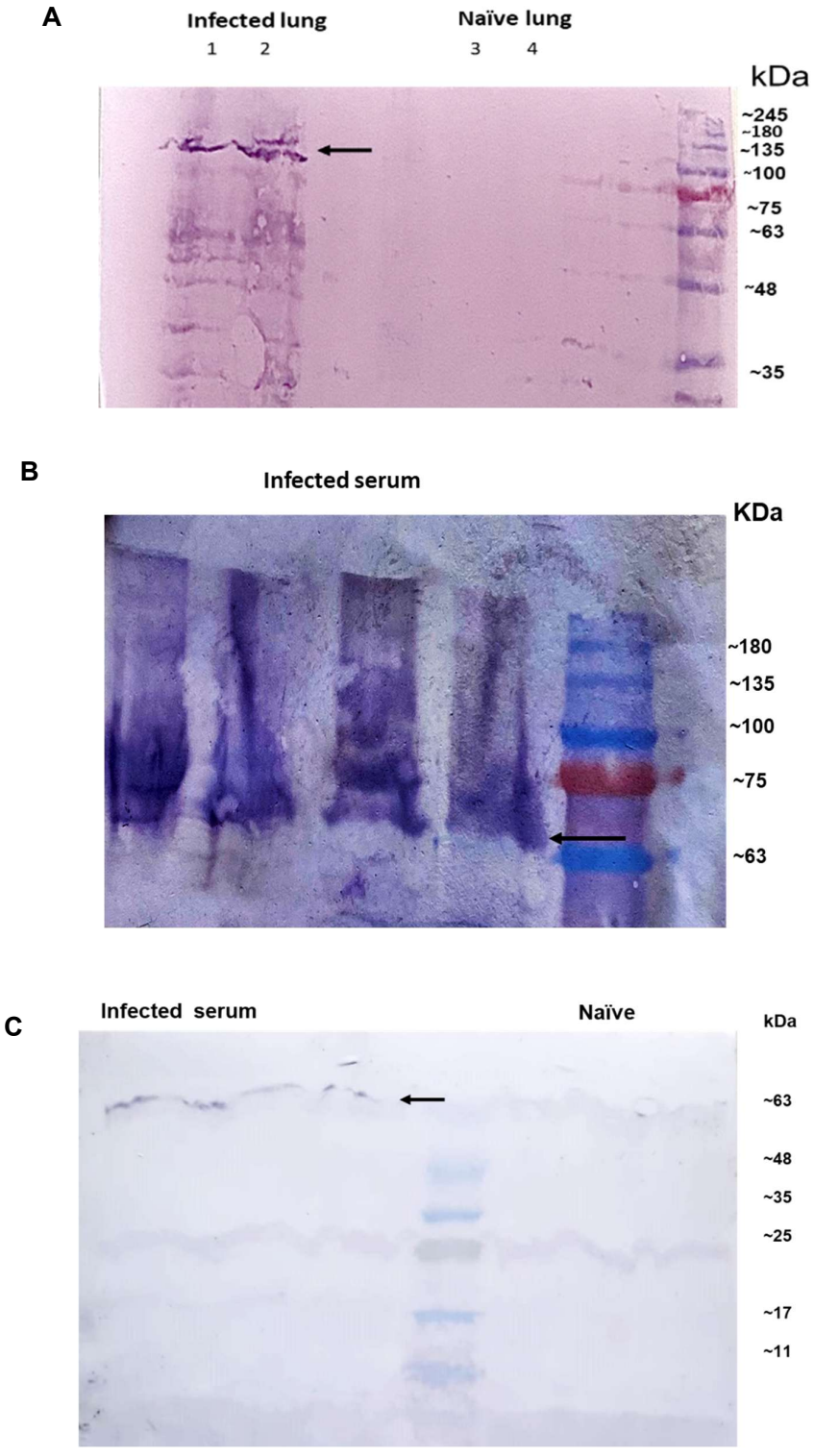

Figure 4: SDS PAGE and Western blot detection of Kex1

RAG-1-/- mice were infected with *P. murina* and samples were collected: lung homogenates (A), and serum (B and C). SDS PAGE and Western blot showing the detection of Kex1.10µl of sample were added to the wells. A protein approximately of 100 kDa was detected in infected lung samples, lanes 1 and 2 (A), with smaller bands corresponding to degradation products being more prominent in serum samples at ~63 kDa (B and C).

A

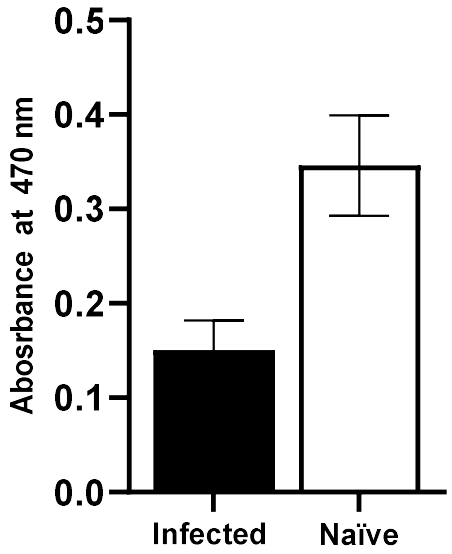

Figure 5: Attempted detection of Kex1 through Indirect ELISA

Lung homogenates were diluted in bicarbonate buffer (1:3) and incubated overnight at 4°C. This was followed by washing 5 times and blocking for 2 hours with 1% PBS/BSA for an hour. One hundred microlitres per well of diluted anti-rabbit secondary antibody conjugated to biotin (1:40 000) was added to the plate and incubated for 2 hours at 25°C, after which the plate was washed 3 times. Streptavidin–HRP was added for 30 mins and the plate was developed with TMB substrate. The absorbance was then measured at 470 nm. The naïve samples indicated higher absorbance.

5.2 Mouse model of *P. murina* and RSV co-infection

Fungal pathogens have been implicated in complicating viral infections, especially in immunocompromised individuals. The immune responses against a fungal pathogen can significantly influence the immune response to a subsequent viral pathogen. RSV is a prevalent cause of lower respiratory tract infections often leading to pneumonia in areas with limited resources. A better understanding of the interaction between *Pneumocystis* and respiratory viruses such as RSV could lead to new therapeutic approaches and clinical improvements in disease management. Thus, the effects of prior *Pneumocystis* infection on the immune response to subsequent RSV challenge in mice were investigated. C57BL/6 wild-type mice and RAG-1-/- mice were infected with *P. murina* and later coinfected with RSV. The infection model was optimised by shortening the time points of RSV infection for later experiments.

To optimise a mouse model of coinfection, mice were infected with *P. murina* and RSV with varying doses of RSV and experimental timelines per experiment. The administration of *P. murina* involved intratracheal instillation of 100 µl containing 2×10^5 cysts while the mice were under anaesthesia. RSV A2 stock generated from Hep-2 cells was used to coinfect the mice and higher doses of RSV [2.5×10^5 PFU (experiment 1), 5×10^5 PFU (experiment 2), or 1.5×10^6 PFU (experiments 3 and 4)] were required to cause disease in mice. For each experimental figure, an experimental design is provided, and three groups of mice were represented, namely: *P. murina* only control group (PcM), RSV only control group, and a *P. murina* and RSV coinfected group. The following disease parameters were investigated: RSV and *P. murina* burden through RT-qPCR, mucus production and tissue inflammatory response through histology staining and imaging, serum antibody production through serum antibody ELISA, and pro-inflammatory cytokine analysis of the lung tissue through cytokine ELISA. The tissue inflammatory response through H&E was not successful due to the difficulty in obtaining quality sections for imaging. Although a plaque assay was attempted to quantify the viral load in lung samples, it proved unsuccessful, with viral levels undetectable in the assay. This may be due to rapid viral degradation. Nonetheless, the assay used to quantify the virus stock was successful; a concentration of 30 million pfu/ml was determined.

5.21 Experiment 1: *P. murina* reduces the RSV burden in C57BL/6 wild-type mice

A mouse model of coinfection was established using C57BL/6 wild-type mice. In experiment 1, mice were infected with 2×10^5 *P. murina* cysts for 14 days. On day 14, they were coinfected with 2.5×10^5 pfu RSV (Fig 6A). Mice were then euthanised 21 days post-*P. murina* infection and disease parameters were measured.

The findings from the qPCR analysis indicated a trend towards reduced RSV burden in the coinfected group compared to the RSV-only group (Fig 6B). The number of RSV copies was very low, this could be due to the lower dose of the intranasal inoculum (2.5×10^5 pfu RSV), technical error during inoculation, or rapid viral degradation. The lung burden of *P. murina* was assessed using both qPCR and GMS staining, with the qPCR data showing a trend towards reduced *P. murina* (Fig 6C). In contrast, *P. murina* was identified through GMS staining in the *P. murina*-only group (Fig 6D). Mucus production through PAS staining was observed in both the coinfected and *P. murina* groups, whereas it was absent in the RSV group (Fig 6D). Cytokine analysis through ELISA showed a trend of increased IL-1β in the *P. murina* control group compared to both the RSV and the coinfected groups, but no differences were observed between groups for other pro-inflammatory cytokines (Fig 7A). Serum antibody analysis revealed significantly increased levels of IgM and IgG in the *P. murina* control group compared to the RSV and coinfected groups (Fig 7B).

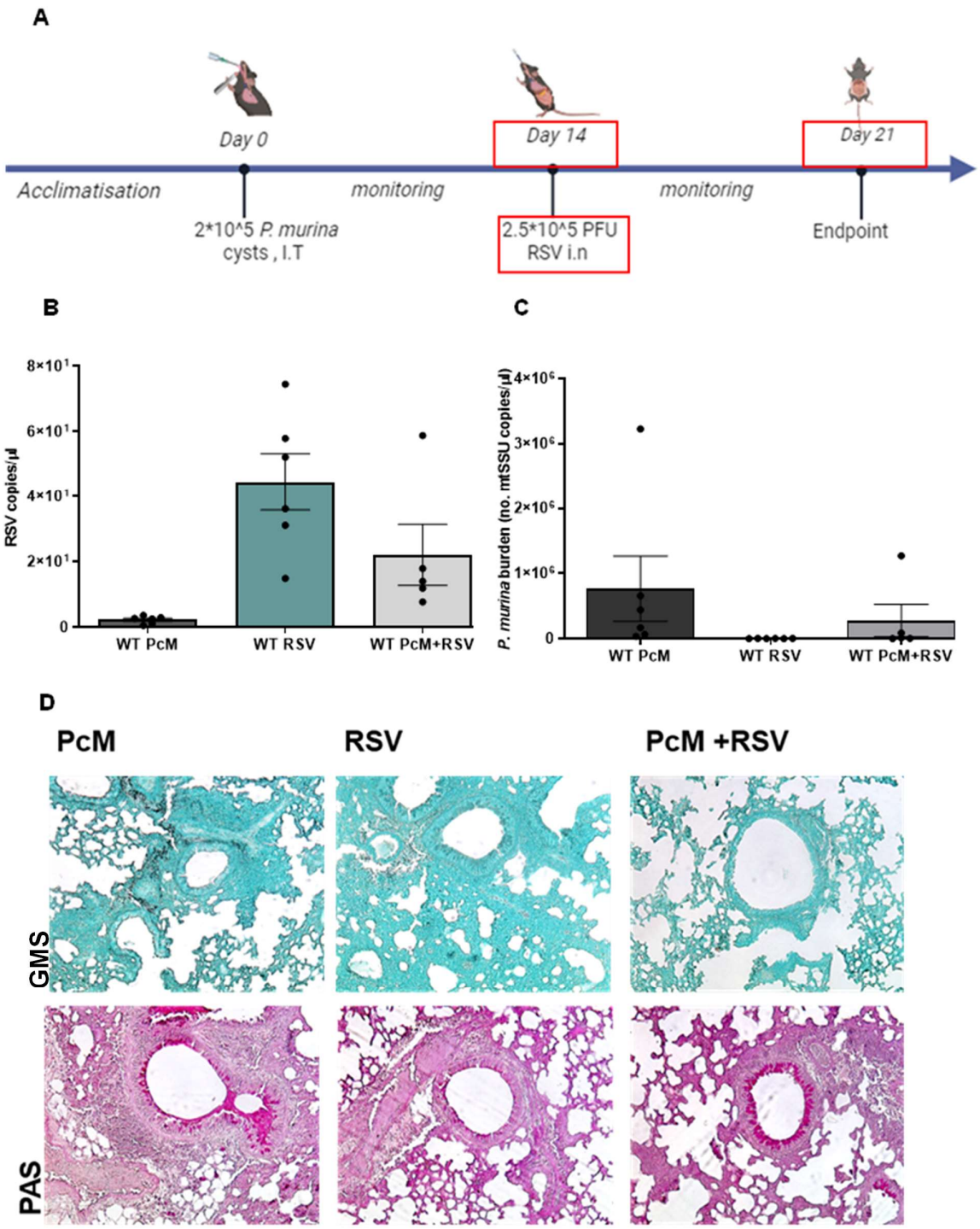

Figure 6: Experiment 1: *P. murina* reduced RSV burden in WT mice.

A) WT mice were infected with 2 × 10^5 *P. murina* cysts for 14 days, and coinfected with 2.5 × 10^5 PFU RSV for an additional 7 days. They were then sacrificed at 21 days post-P. *murina* infection. B) RSV burden by RT-qPCR. C) *P. murina* by qPCR. D) *P. murina* visualisation and mucus production by GMS and PAS staining, respectively (20x magnification). Differences across groups were analysed using one-way ANOVA with multiple comparison tests; each bar represents the mean ±SEM of 6 mice. Data represents 1 experiment.

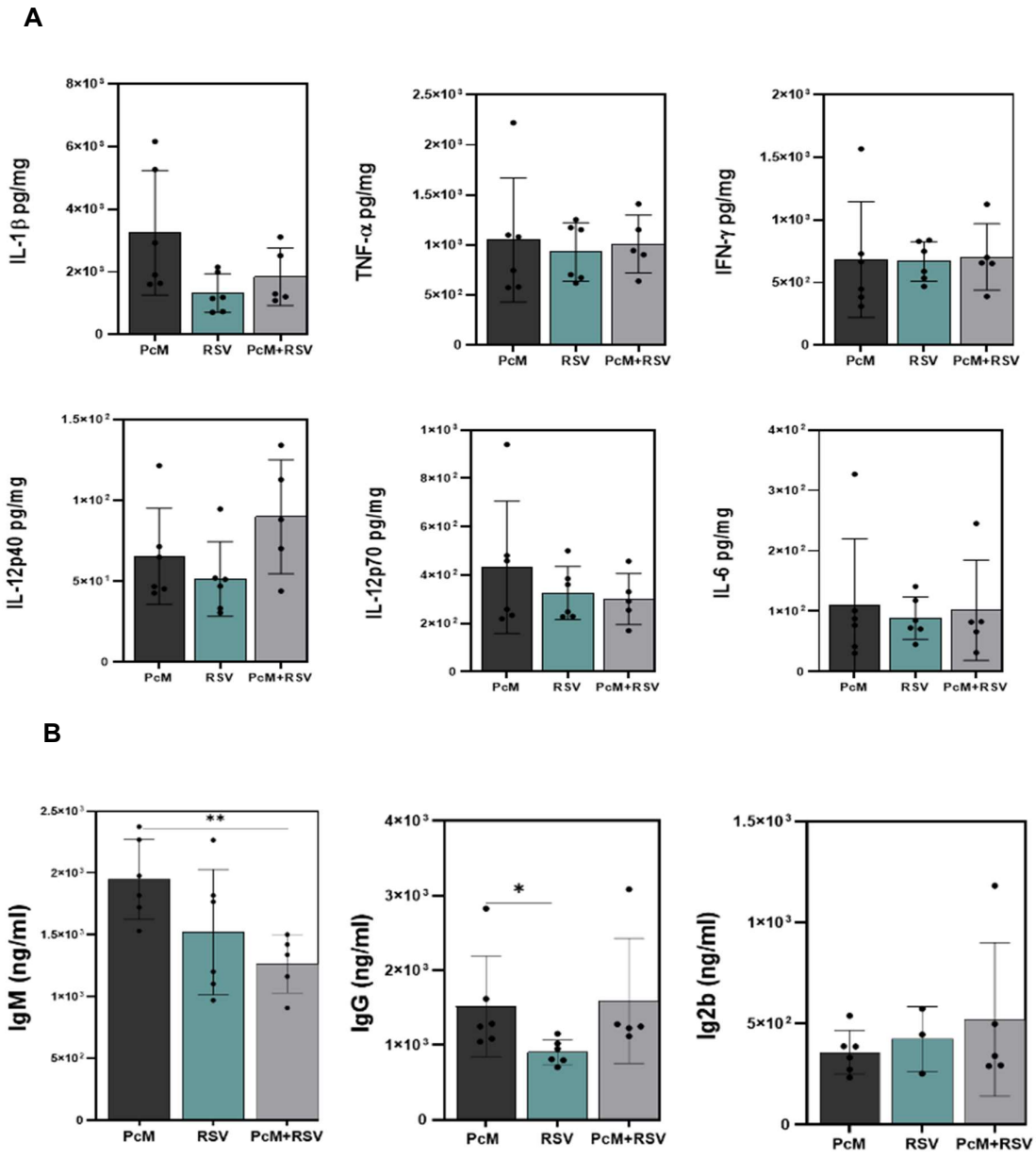

Figure 7: Experiment 1, Lung cytokine and serum antibody analysis.

E) Cytokines measured by ELISA show a trend towards increased IL-1β in the PcM group compared to the RSV and the coinfected group. F) Serum antibodies measured by ELISA indicated significantly elevated levels of IgM and IgG in the PcM group compared to the RSV and the coinfected group. Data points for Ig2b are missing because they were below the standard curve range. Each bar graph represents the mean± SD of 6 mice. Differences across groups were analysed student by one-way ANOVA with multiple comparison tests; p=0.05: *; p=0.01: **; p=0.001: ***. PcM= *P. murina*. Data represents 1 experiment

5.22 Experiment 2: *P. murina* burden significantly reduces RSV in C57BL/6 wild type mice

The subsequent experimental timeline (Experiment 2) was shortened to ascertain whether any differences would emerge when the *P. murina* lung burden was anticipated to be higher. RSV is not a mouse pathogen, and higher doses are required to cause disease in mice. This was evident from Experiment 1, where RSV was on the limit of detection by qPCR. In Experiment 2, the RSV dose was increased twofold. In this experiment, WT mice were infected with 2×10^5 *P. murina* cysts for 7 days. On day 7 of the infection, the mice were coinfected with a twofold increase in RSV (5×10^5 pfu RSV) and subsequently euthanised 14 days post-*P. murina* infection (Fig 8A).

With these time points of infection, and in the presence of a 2-fold increased dose of RSV, there was a significantly reduced RSV burden in the coinfected group compared to the RSV-only group (Fig 8B). The *P. murina* lung burden was not significantly different between the coinfected group and the *P. murina* as seen through qPCR (Fig 8C). It was difficult to distinguish cysts by GMS staining at this time point (Fig 8C). Mucus production through PAS staining was observed in both the coinfected and *P. murina* groups, whereas it was absent in the RSV group (Fig 8D). There were no significant differences observed in the relative mRNA levels of IFN-β (Fig 9A). The following pro-inflammatory cytokines were found to be significantly elevated in the *P. murina* group compared to the RSV group and coinfected group: IL-1β, TNF-α, IFN-γ, IL-12p40, and IL-12p70 (Fig 9B). Significantly elevated serum antibody levels were observed in the *P. murina* control group for both IgM and Ig2b compared to the RSV and coinfected groups (Fig 10A).

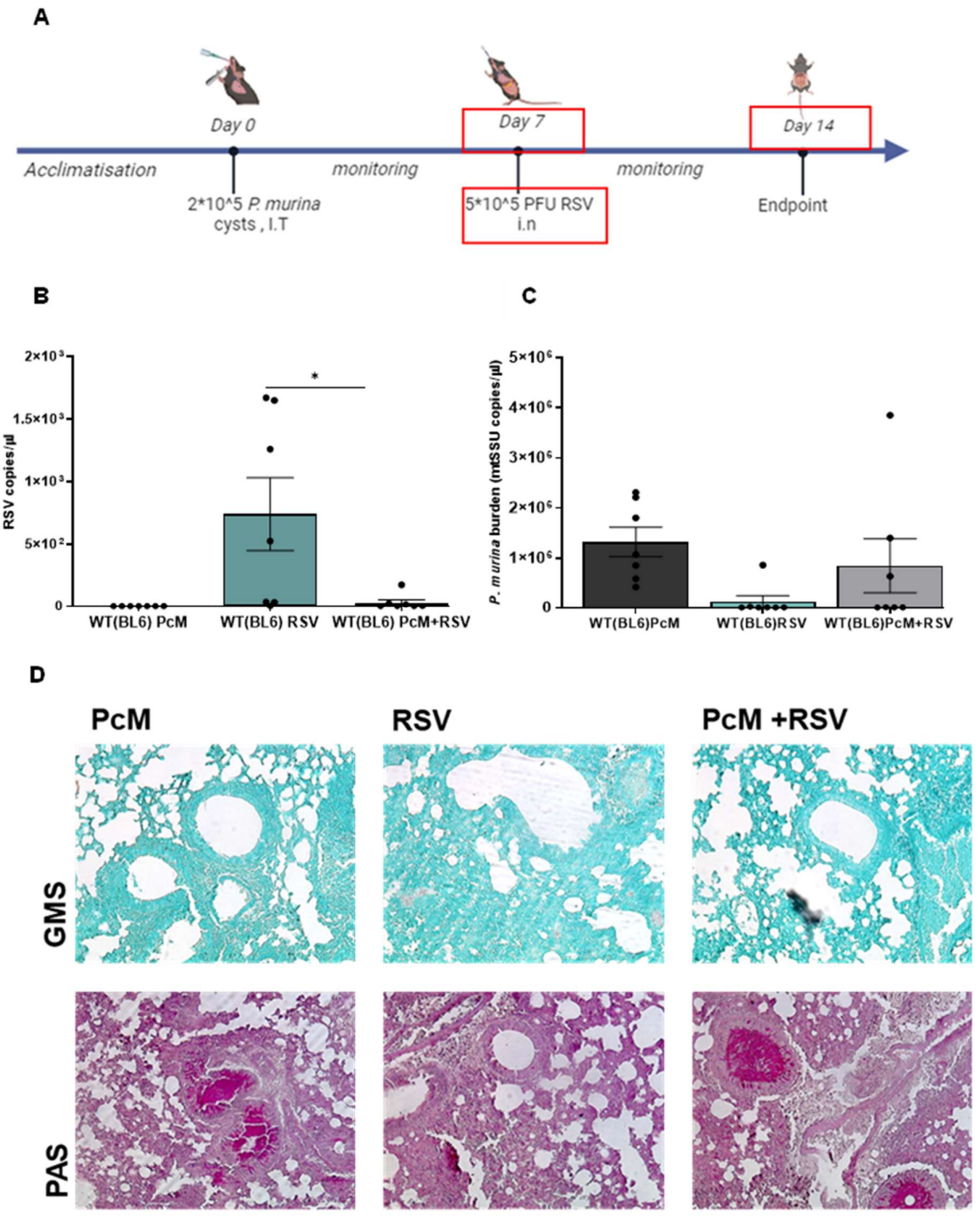

Figure 8 :High *P. murina* burden significantly reduces RSV burden in WT mice

WT mice were infected with 2 × 10^5 *P. murina* cysts for 7 days, and coinfected with 5 × 10^5 PFU RSV for an additional 7 days. They were then sacrificed at 14 days post *P. murina* infection. A) Experimental layout. B) RSV burden by RT-qPCR. C) *P. murina* by qPCR. D) *P. murina* visualisation and mucus production by GMS and PAS staining, respectively (20x magnification). Mucus production is evident in the PcM and coinfected groups but not in the RSV group. Differences across groups were analysed using one-way ANOVA with multiple comparison tests. Each bar represents mean ±SEM of 7 mice per group; p=0.05: *; p=0.01: **; p=0.001: ***. PcM= *P. murina*. The data represents 1 experiment.

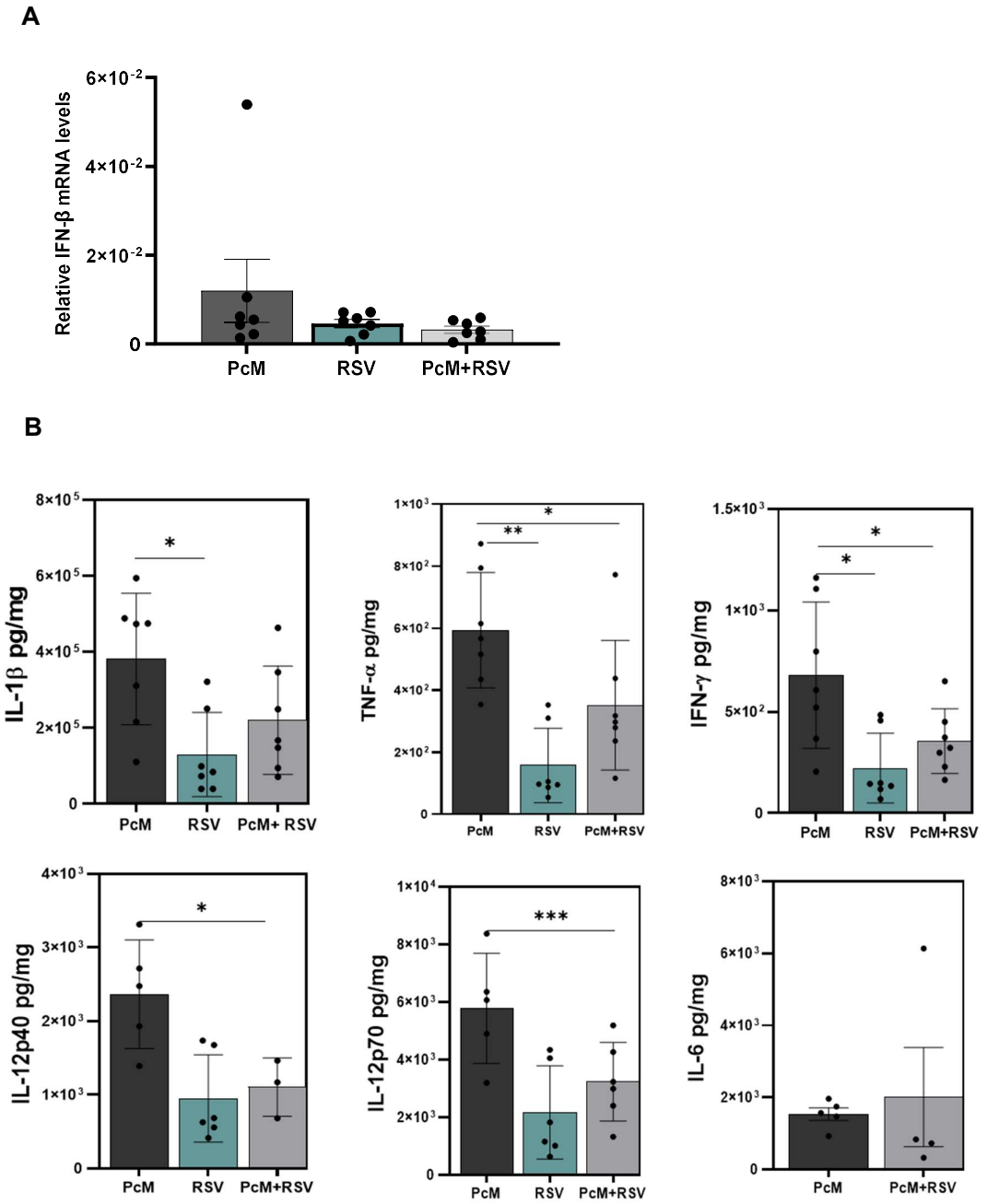

Figure 9 : Experiment 2, Lung IFN-β and cytokine analysis.

A) Type I interferons measured by relative quantification of IFN-β mRNA and analysed by One-way ANOVA using the Brown–Forsythe test. There were no significant differences in the levels of IFN-β across the groups. B) Pro-inflammatory cytokines measured by ELISA indicated significantly elevated levels of IL-1β, TNF-α, and IFN-γ, in the PcM group compared to the RSV group. IL-6 was not detected in the RSV group; some of the data points were below the standard curve range. Each bar graph represents the mean±SD of 7 mice. Differences across groups were analysed using one-way ANOVA with multiple comparison tests; p=0.05: *; p=0.01: **; p=0.001: ***. PcM= *P. murina*. The data represents 1 experiment.

A

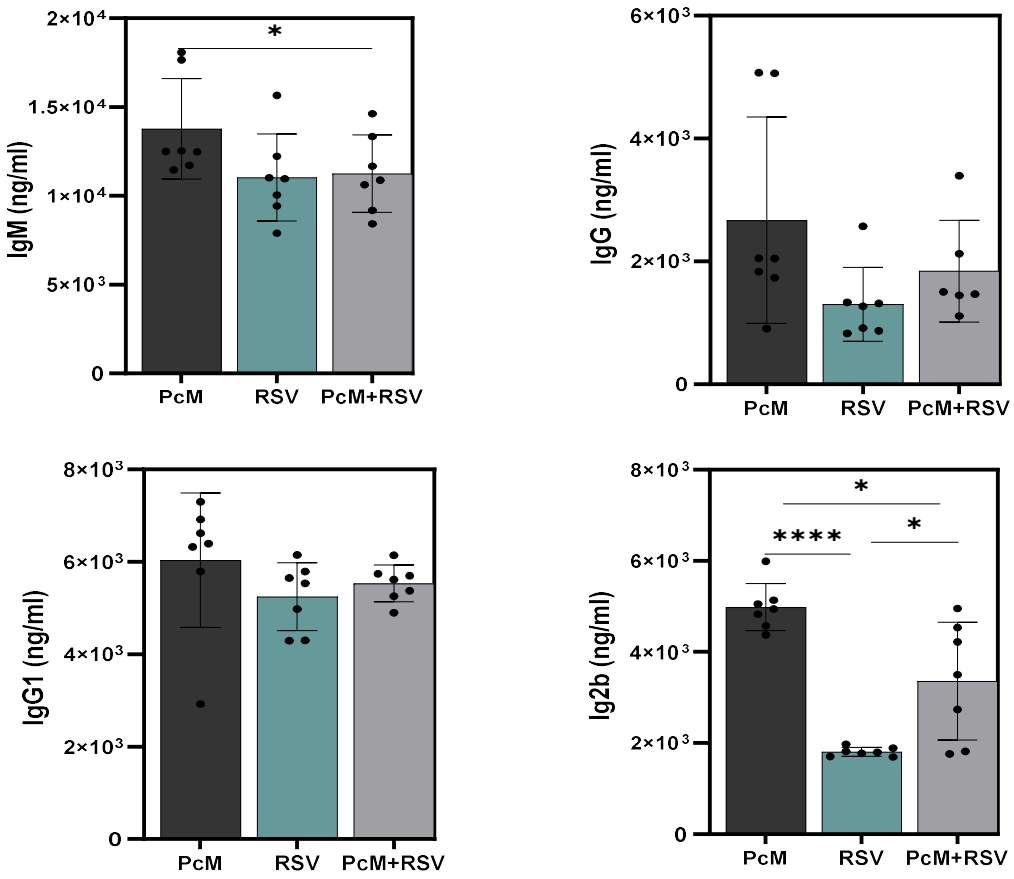

Figure 10: Experiment 2, serum antibody analysis.

A) Serum antibodies measured by ELISA. The levels of IgM and Ig2b were significantly elevated in the PcM group compared to the RSV and coinfected groups. Each bar graph represents the mean± SD of 7 mice. Differences across groups were analysed by one-way ANOVA with multiple comparison tests; p=0.05: *; p=0.01: **; p=0.001: ***. PcM= *P. murina.* The data represents 1 experiment.

5.23 Experiment 3: *P. murina* reduced the RSV burden in C57BL/6 wild-type mice during peak RSV viral replication.

To further explore whether there would be variations in RSV levels during the peak of viral replication mice were infected with *P. murina* and coinfected with RSV, then euthanised during peak RSV replication. In humans, the peak of RSV replication is estimated to occur between days 4 and 6 of infection. In experiment 3, C57BL/6 wild-type mice were infected with 2×10^5 *P. murina* cysts for 7 days and then coinfected with 1.5×10^6 pfu RSV for 4 days, with the fourth day of RSV coinciding with the peak viral load (Durbin et al. (2002) ;Jafri et al. (2004)) (Fig 11A). The mice were euthanised 11 days post *P. murina* infection.

The qPCR results demonstrated that during the period of peak viral replication, the mice that had been coinfected with *P. murina* and RSV exhibited a clearance of RSV (Fig 11B). *P. murina* lung burden was elevated in the *P. murina* group (Fig 11C). However, this was not clearly evident through GMS staining since day 7 of *P. murina* is too early to observe the cysts in the lung tissue (Fig 11D). Mucus production through PAS staining was observed in both the coinfected and *P. murina* groups, whereas it was absent in the RSV group (Fig 11D). The analysis of IFN-β indicated significantly elevated levels of this cytokine in the RSV control group in comparison to the coinfected group and the *P. murina* control group (Fig 12A). Similarly, the levels of IL-1β, IL-12p40, IL-12p70, and IL-6 were markedly elevated in the *P. murina* control group compared to the RSV group (Fig 12B), and the levels of IL. The levels of IFN-γ could not be measured as they were below the standard curve range limit. The following serum antibody levels were found to be elevated in the *P. murina* group compared to the RSV group: IgG, IgG1, Ig2b, and IgM (Fig 13A).

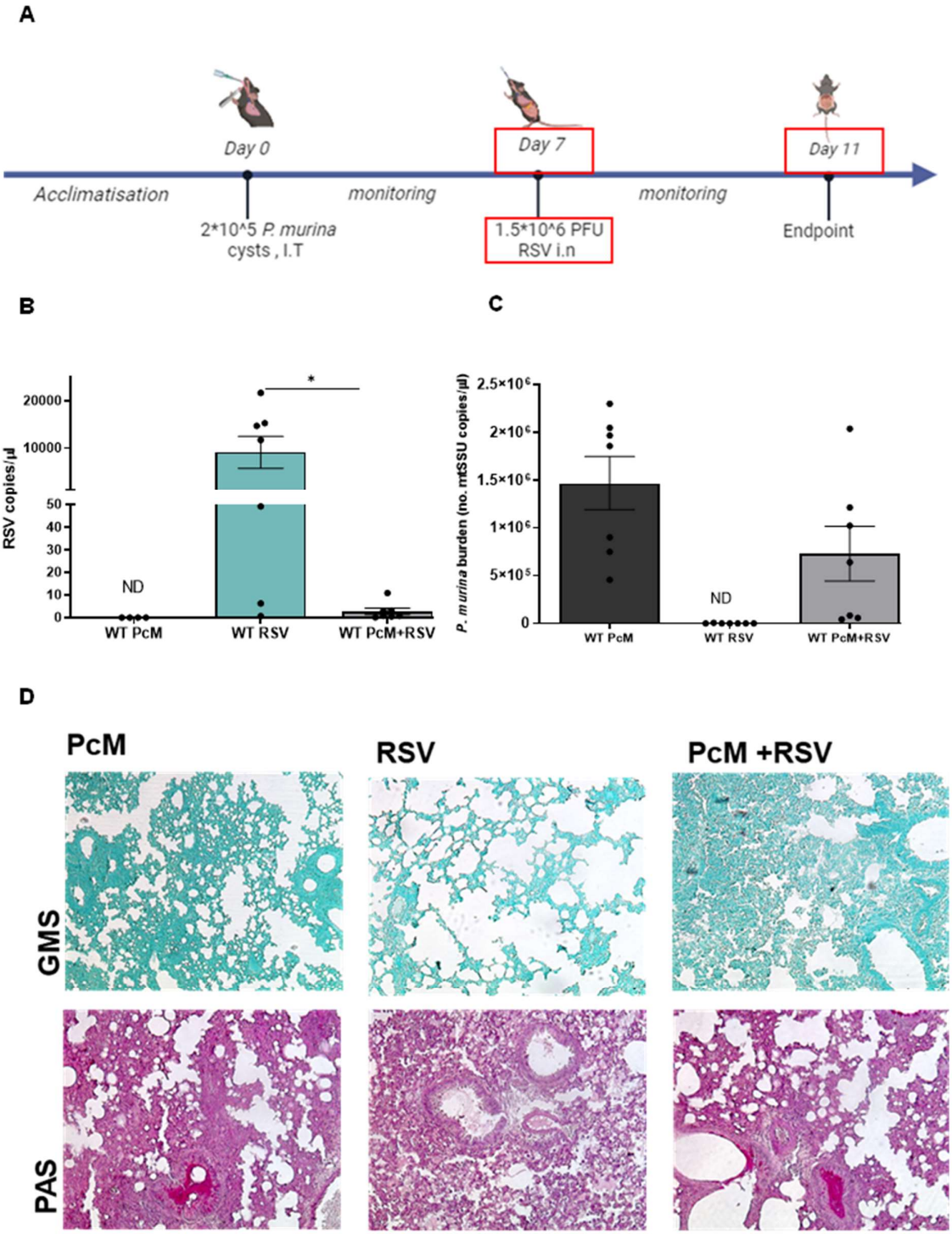

Figure 11: Experiment 3. *P. murina* reduces RSV burden during the peak of viral replication.

WT mice were infected with 2 × 10^5 *P. murina* cysts for 7 days, and coinfected with 1.5 × 10^6 PFU RSV for an additional 7 days. They were then sacrificed at 14 days post *P. murina* infection. A) Experimental layout. B) RSV burden by RT-qPCR. C) *P. murina* by qPCR. D) *P. murina* visualisation and mucous production by GMS and PAS staining, respectively (20x magnification). Mucus is evident in the PcM and coinfected groups but not in the RSV group. Differences across groups were analysed using one-way ANOVA with multiple comparison tests. Each bar represents mean ±SEM of 7 mice per group; p=0.05: *; p=0.01: **; p=0.001: ***. PcM= *P. murina*, ND=non detected. The Data represents 1 experiment

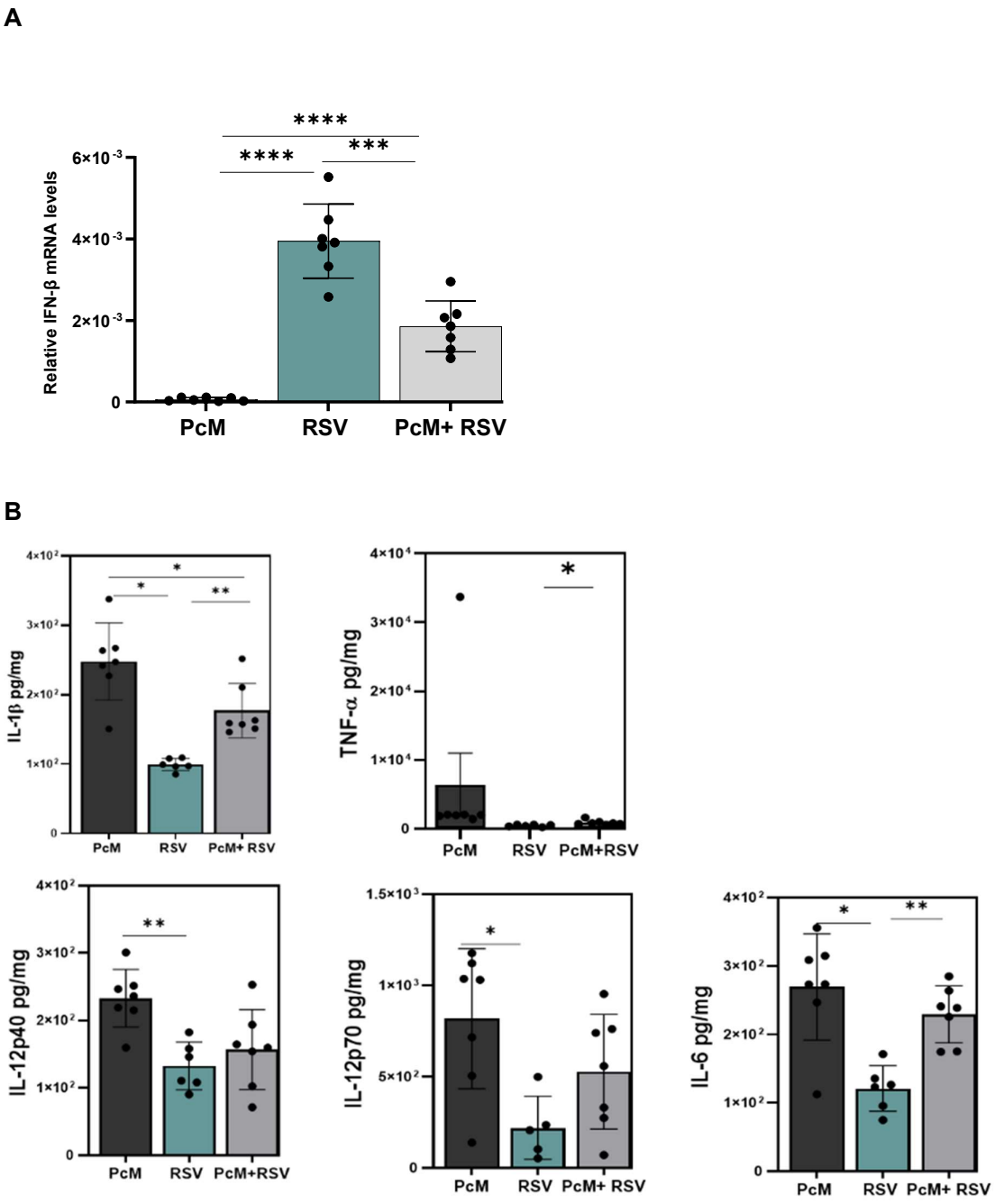

Figure 12: Experiment 3, Lung cytokine and serum antibody analysis.

A) Type I interferons measured by relative quantification of IFN-β mRNA and analysed by one-way ANOVA with multiple comparison tests. The levels of IFN-β are significantly elevated in the RSV group compared to the PcM and the coinfected groups. B) ELISA measured pro-inflammatory lung cytokines. The pro-inflammatory cytokines IL-1β, IL-12p40, IL-12p70, and IL-6 were significantly elevated in the PcM group, compared to the RSV group. The levels of IFN-γ were also measured but were below the standard curve range. Each bar graph represents the mean±SD of 7 mice. Differences across groups were analysed student by student T-test; p=0.05: *; p=0.01: **; p=0.001: ***. PcM= *P. murina*. The Data represents 1 experiment.

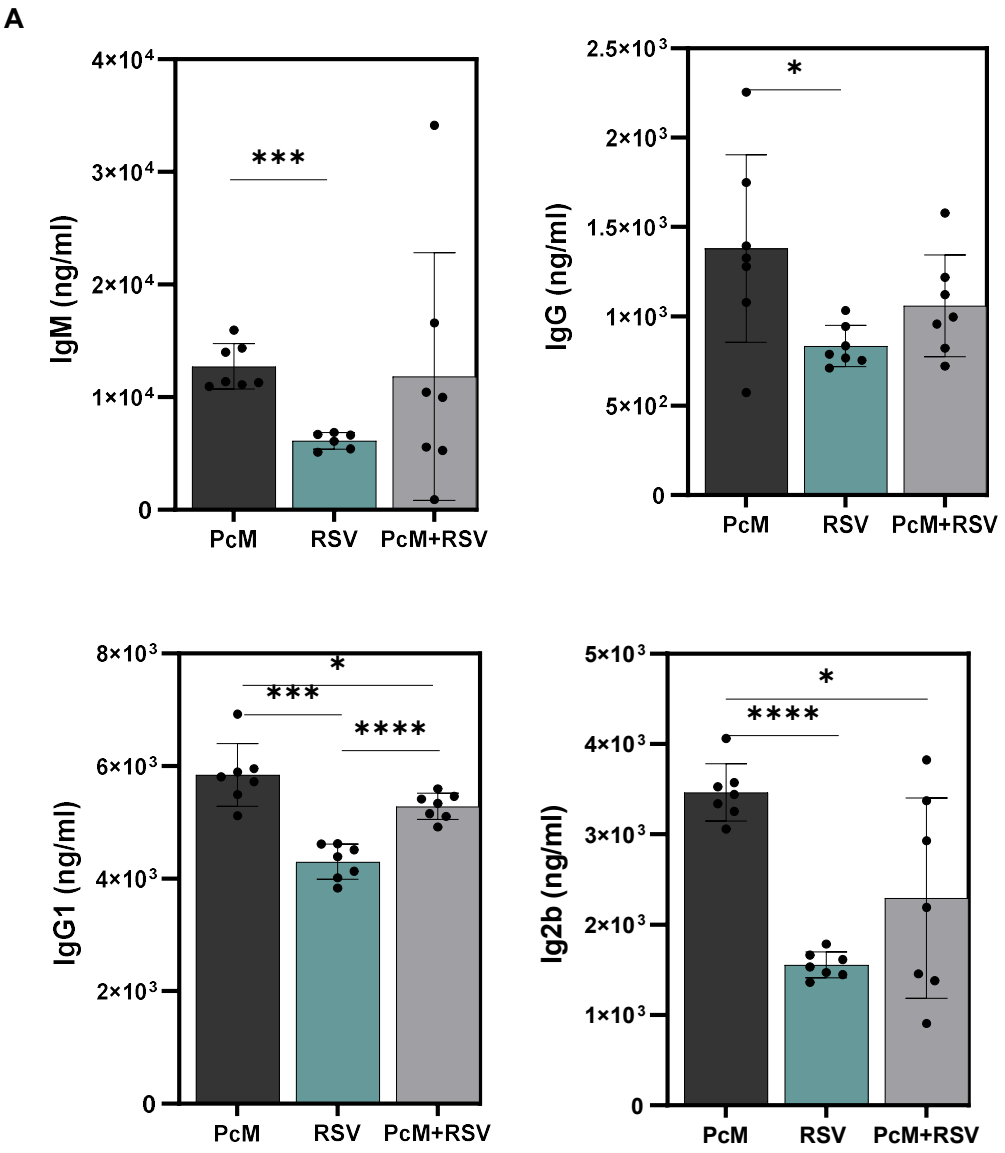

Figure 13: Experiment 3, Serum antibodies during the peak of RSV replication.

A) Serum antibodies measured by ELISA indicated significantly elevated levels of IgM, IgG, IgG1, and Ig2b in the PcM group relative to the RSV group. Each bar graph represents the mean± SD of 7 mice. Differences across groups were analysed student by one-way ANOVA with multiple comparison tests; p=0.05: *; p=0.01: **; p=0.001: ***. PcM= *P. murina*. The Data represents 1 experiment.

5.24 Experiment 4: *P. murina* reduced the RSV burden in RAG -1 -/- mice during peak viral replication

Finally, to determine if the effects of coinfection differ in immunocompromised mice, RAG1-deficient mice were also subjected to infection with 2×10^5 *P. murina* cysts for 7 days, followed by a 4-day coinfection with 1.5×10^6 pfu RSV (Fig 14A). These mice were euthanised 11 days post *P. murina* infection, and various disease parameters were evaluated. RAG1-deficient mice are characterised by the absence of the RAG1 protein, which is essential for the recombination of variable (V), diversity (D), and joining (J) segments of immunoglobulin and T cell receptor (TCR) genes (Bosticardo et al., 2021). Consequently, the deficiency of RAG1 proteins and the associated TCR genes leads to a complete absence of mature T and B lymphocytes in these mice, rendering them incapable of activating an adaptive immune response and making them susceptible to severe infections.

Similar to WT mice, in immunocompromised RAG1-deficient mice it was observed that *P. murina* reduced the RSV burden (Fig 14B). Neither the *P. murina* organisms through GMS nor mucus production through PAS staining was evident in any of the groups (Fig 14D). The levels of IFN-β were significantly elevated in the RSV-only group compared to the *P. murina* group (Fig 15A). Although not statistically significant, there was a discernible trend towards elevated levels of IL-1β, TNF-α, and IL-12p70 in the *P. murina* group compared to the RSV group (Fig 15B). It is noteworthy that while IL-6 levels were significantly elevated in the RSV-only group, they were undetectable in the *P. murina* group (Fig 15B).

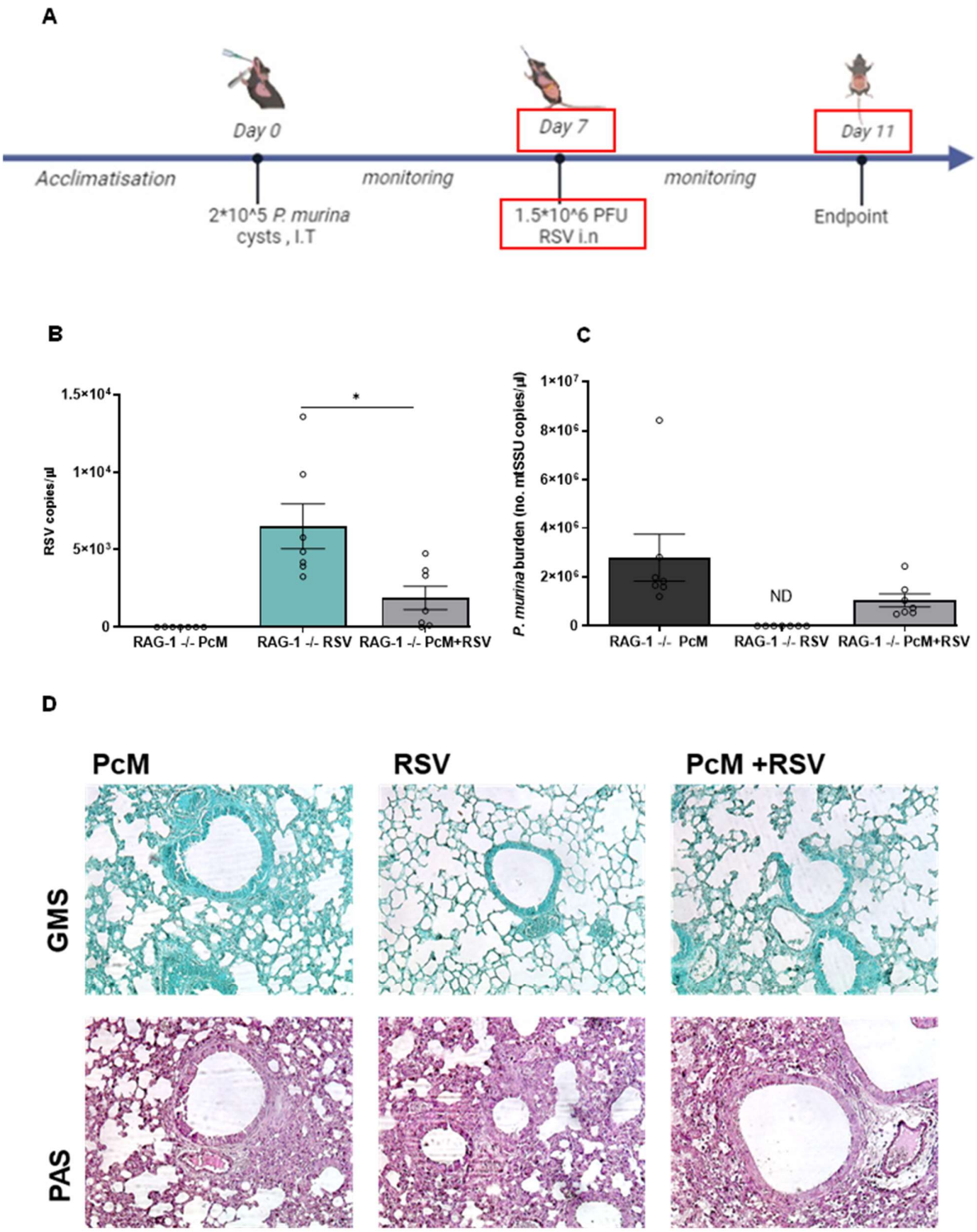

Figure 14: *P. murina* reduces RSV burden in RAG-1 -/- mice.

RAG1-deficient mice were infected with 2 × 10^5 *P. murina* cysts for 7 days, and coinfected with 1.5 × 10^6 PFU RSV for an additional 7 days. They were then sacrificed at 14 days post *P. murina* infection. A) Experimental layout. B) RSV burden by RT-qPCR. C) *P. murina* by qPCR. D) *P. murina* visualisation and mucous production by GMS and PAS staining, respectively (20x magnification). Differences across groups were analysed using one-way ANOVA with multiple comparison tests. Each bar represents mean ±SEM of 7 mice per group; p=0.05: *; p=0.01: **; p=0.001: ***. PcM= *P. murina*. The data represents 1 experiment.

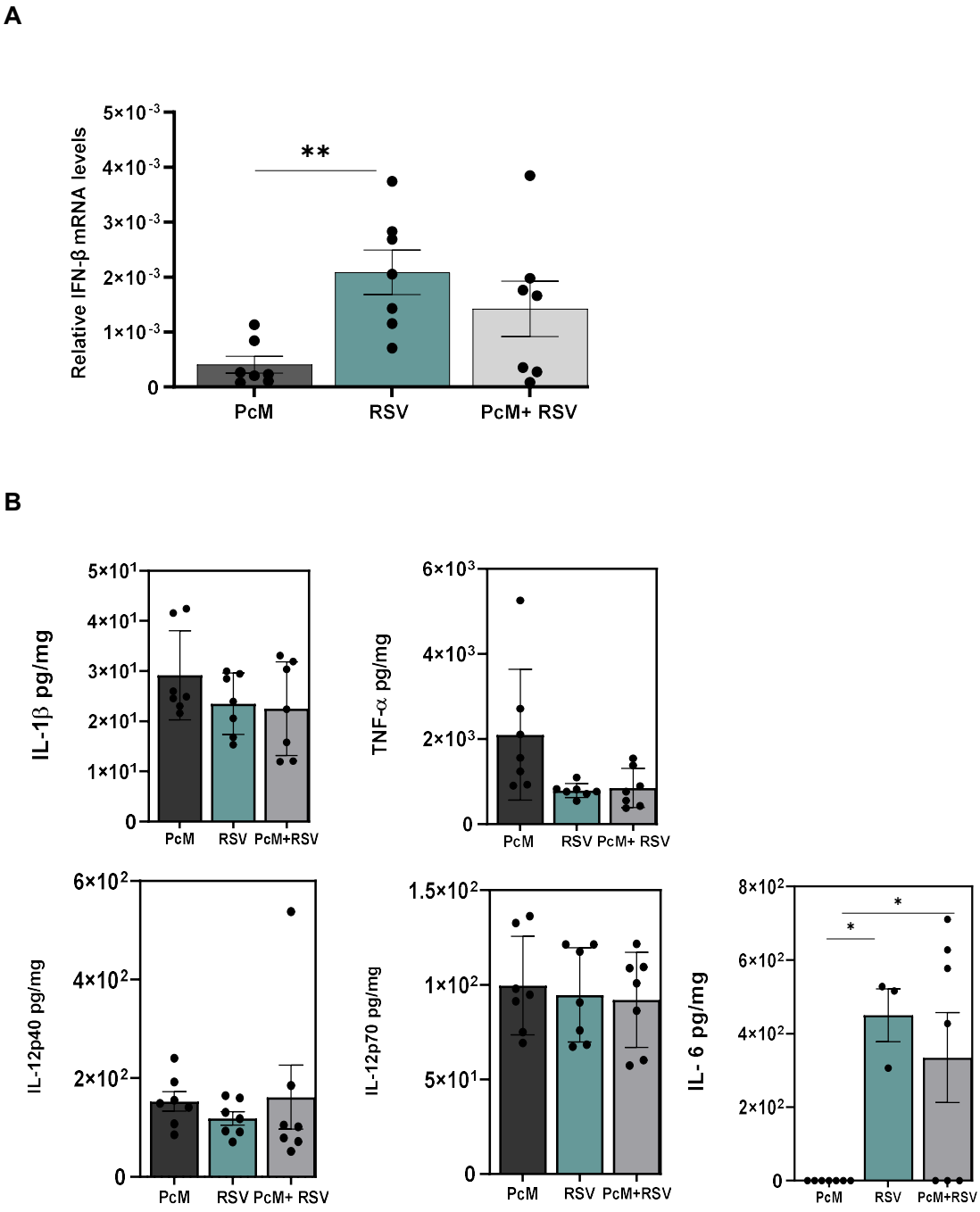

Figure 15 : RAG-1 -/- IFN-β and lung cytokines analysis.

A) Type I interferons measured by relative quantification of IFN-β mRNA and analysed by One-way ANOVA using the Brown–Forsythe test. The levels of IFN-β were significantly elevated in the RSV group compared to the PcM group. B) Pro-inflammatory lung cytokines measured by ELISA. Results indicate a trend towards increased IL-1β and TNF-α in the PcM group compared to the RSV group. The levels of IL-6 were significantly elevated in the RSV group compared to the PcM group. Each bar graph represents the mean± SD of 7 mice. Differences across groups were analysed student by one-way ANOVA with multiple comparison tests; p=0.05: *; p=0.01: **; p=0.001: ***. PcM= *P. murina*. The Data represents 1 experiment.

6. Discussion

6.1 Detection of Kex1 in samples from *P. murina*-infected mice

Despite the advances made in understanding *P. jirovecii*, it cannot be reliably cultured *in vitro*, making diagnosis difficult. Hence, the current methods of diagnosis are through invasive and expensive techniques using BAL and induced sputum, the current gold standard. The use of these methods is not always feasible in low-resource settings, for children, patients with respiratory distress, and those who are hypoxic. Additionally, the current methods of diagnosis cannot differentiate between colonisation and current infection. With the rise of PCP in non-HIV-infected patients, there is a demand for reliable, non-invasive, inexpensive, and easy-to-use techniques for the rapid point-of-care diagnosis for PCP. The use of patient samples such as blood, along with antibodies directed at cell surface proteins found in *P. jirovecii* have gained attention as alternative methods of diagnosis.

Serological metabolites such as β(1,3)-glucan, LH, KL-6, and SAM have been associated with PCP. However, their specificity for *P. jirovecii* is limited, and the diagnostic cut-off values remain ambiguous. Recent investigations have focused on the reactivity of antibodies against *Pneumocystis* proteins, such as MSG and Kex1, as potential immunological markers for the disease (Tomás et al. (2016); Tomás et al. (2019)). Vaccination with Kex1 has demonstrated protective properties, and the encoding by a single nuclear copy gene (PRTT1) enhances its reliability as a serological biomarker compared to MSG (Kutty and Kovacs (2003); Cobos Jiménez et al. (2019)). In this study, we evaluated the presence of Kex1, a conserved surface protein in *Pneumocystis* species, for the rapid diagnosis of PCP using an immunoassay. The Kex1 antiserum was applied to infected mouse lung homogenates, urine, and serum. Utilising a dot-blot technique, which preserves the native structure of proteins, we successfully detected Kex1 in lung homogenates, urine, and serum. Kex1 was readily detectable by dot blot of native protein samples. This may be attributable to the fact that the polyclonal antiserum may contain antibodies which only recognise epitopes from native proteins and thus have higher chances of binding during a dot blot compared to a Western blot. The presence of Kex1 in urine and serum samples could indicate the release of Kex1 from *P. murina* organisms in the lung into the bloodstream during the course of infection. The detection of Kex1 in both urine and serum provides evidence for the potential as a non-invasive diagnostic tool for PCP. Additionally, through SDS-PAGE and western blot analysis, we established that the molecular weight of Kex1 in lung samples is approximately 100 kDa, with smaller bands indicative of degradation products observed around 63 kDa, with these degradation products correspond

to the molecular weight of Kex1 observed in serum samples. The size of *P. murina* Kex1, as predicted from the 3.1 kb cDNA, was 1011 amino acids, corresponding to a theoretical size of 112 kDa (Lee et al., 2000). The differences in molecular weight between lung and serum samples could be due to the addition of a protease inhibitor in the lung samples only. The use of a protease inhibitor reduces protein degradation and results in a higher intact protein yield. Alternatively, Kex1 in the bloodstream may have undergone degradation before sample collection. The proof-of-concept experiment was successful in detecting Kex1 from *P. murina*-infected mice. It should be noted that protein samples in this study were obtained from mice which were heavily infected and euthanised at the end stage of the disease, where the fungal burden was expected to be high. The results in comparison to human samples may vary, where the fungal burden might be lower, and the difference between colonisation and infection might be challenging. To counteract this difficulty, a semiquantitative real-time PCR can be employed to distinguish between colonisation and infection (Grønseth et al., 2021).

This study further explored the detection of Kex1 through an indirect ELISA, in which high non-specific binding of Kex1 in the naïve samples was observed. For indirect ELISA, a primary antibody is exposed to an antigen, which is then exposed to a secondary antibody. Non-specific binding by either antibody to the sample, which is directly adsorbed to the surface of the plate, can occur, as observed in our study, especially if blocking was not sufficient. The increased number of reagents used in biotin-streptavidin-HRP detection chemistry can also contribute to high background signalling. The results could be improved by increasing the blocking buffer concentration and optimising the blocking time. To mitigate non-specific binding, the implementation of a sandwich ELISA may be considered, as this approach is more specific due to its requirement for two antibodies to identify the target of interest.

6.2 The effects of *P. murina* on subsequent RSV infection

Respiratory syncytial virus is a prevalent etiological agent of pneumonia in children younger than 5. Serological investigations have revealed that most individuals would have developed antibodies to *P. jirovecii* by age 4 (Pifer et al., 1978). This suggests prior exposure or infection. It is plausible that RSV and *P. jirovecii* may co-infect a host, leading to pneumonia during early childhood. This co-infection may induce co-signalling mechanisms that confer protection or exacerbate disease severity, contingent upon the host's immune response. In this study, we investigated the effects of *P. murina* on RSV by employing various doses of RSV at multiple experimental timelines. The effects were assessed in both WT mice, representing healthy hosts, and RAG1-deficient mice, which serve as a model for immunocompromised hosts.

In contrast to the negative effects typically linked to coinfections, our study indicates a positive outcome for the host. In C57BL/6 wild-type mice, it was observed that *P. murina* reduces the RSV burden in coinfected mice. This reduction correlated with mucus production in the coinfected group (by PAS staining), which was absent in the RSV-only group. While the mucus production was not quantified, we could hypothesise the involvement of Th2-mediated immune responses, which play a critical role in driving mucus production and result in entrapping pathogens in the respiratory tract (Cohn et al., 1999). Additionally, analysis of the *P. murina* lung burden suggested a trend towards lower levels of *P. murina* in the coinfected group compared to the control group. This finding is further corroborated by GMS staining, which identified *P. murina* cysts exclusively in the *P. murina* control group (Experiment 1, Fig 6D). The reduction of *P. murina* in the coinfected group could be explained by the fact that both *Pneumocystis* and RSV use Type 1 pneumocytes to replicate. There could be competitive binding or some form of microbial interference. Microbial interference has been described during coinfections as one pathogen occupying a niche that prevents the colonisation of another pathogen (Brogden et al., 2005). In experiment 2 (Fig. 8C) specifically, there was complete *P. murina* sterilisation in 4/7 WT mice that were coinfected with RSV compared to those solely infected with *P. murina*. This complete *P. murina* "sterilisation" was not observed in coinfected RAG mice. This phenomenon may be attributed to the fact that a small lobe was sampled for PCR. The zero copies detected for some mice may not necessarily mean it was cleared from the whole lung. Additionally, WT mice possess a more effective ability to eliminate *P. murina* due to their adaptive immune response, which is lacking in RAG mice.

IFN-β functions as an antiviral cytokine that induces an antiviral state in alveolar epithelial cells and facilitates the secretion of various pro-inflammatory cytokines, such as IL-6, TNFα, and IL-1β. Notably, our study indicated that the coinfected group exhibited a lower viral load and correspondingly reduced levels of IFN-β when compared to the RSV control group. This observation suggests a decrease in viral replication within the coinfected group relative to the RSV group. Increased levels of IFN-α/β have been associated with increased disease severity and recurrent wheezing (Tabarani et al. (2013); Vázquez et al. (2019)). Furthermore, the levels of the pro-inflammatory cytokines IL-1β, TN-α, IL-12 p40 and p70 in WT mice were reduced in the RSV group compared to the *P. murina* group and the coinfected groups. In WT mice, the levels of pro-inflammatory cytokines IL-1β, TNFα, IL-12 p40, and p70 were reduced in the RSV group compared to both the *P. murina* group and the coinfected groups. IL-1β was consistently elevated in all the experiments in our study. Moreover, IL-1β has been implicated in trained immunity (Moorlag et al., 2018). During trained immunity, the innate immune cells are reprogrammed in a way that exposure to a secondary pathogen is more robust (Netea et al., 2020). This phenomenon is exemplified by BCG vaccination, where enhanced IL-1β

expression correlated with reduced circulating levels of the yellow fever vaccine virus (Arts et al., 2018). The findings in this study imply that the reduced RSV burden in the coinfected group was influenced by the pro-inflammatory cytokines elicited by the primary *P. murina* infection. A similar pattern of pro-inflammatory cytokine levels was observed in RAG1-deficient mice. In contrast, the levels of IL-6 were significantly elevated in the RSV group compared to both the *P. murina* and coinfected groups (Experiment 4, Fig 15B). Increased levels of IL-6 during RSV infections are associated with increased disease severity (Hornsleth et al., 1998). The levels of IL-6 have been reported to be elevated in SCID mice infected with *P. murina*, as well as in immunocompromised patients with PCP (Chen et al. (1993); Iriart et al. (2010)). Conversely, another study reported reduced levels of IL-6 in the BAL of PCP patients with AIDS compared to those without AIDS (Tasaka et al., 2010). In our study, the levels of IL-6 in *P. murina*-infected mice were low. This could have been due to a technical error during the assay procedure. The values were not detectable because they were below the standard curve range. Furthermore, IL-6 responses in RAG1-deficient mice are equivalent or stronger than those of WT mice in response to viruses (Percopo et al. (2017);Percopo et al. (2019)), but weaker for other pathogens like *Cryptococcus neoformans* (Dufaud et al., 2018).

The rapid viral clearance in the coinfected WT mice may be associated with increased antibody response. Specifically, the antibodies IgM, IgG, IgG1 and IgG2b. IgM antibodies are typically present during the acute phase of infection, playing a crucial role in the initial antibody response to pathogens. In the context of *Pneumocystis* infection, these antibodies facilitate a dendritic cell response and are essential for eliciting Th2 and Th17 responses (Rapaka et al., 2010). In infants, the presence of pre-existing antibodies during RSV infection significantly influences the immune response, with lower levels of neutralising antibodies associated with increased lower respiratory tract infection rates (Freitas et al., 2011). Following the production of IgM antibodies, IgG antibodies emerge, indicating a more advanced and specific immune response (Albarbar, 2024). Additionally, IgG antibodies enhance viral clearance through mechanisms such as opsonisation, neutralisation of antigens, and activation of the classical complement pathway (Hamilton, 1987). These antibodies have been shown to appear 2 weeks post-RSV infection, reaching maximum titres during week 4 of infection (Hornsleth et al., 1985). The monoclonal human recombinant IgG1 antibody Nirsevimab is said to be protective against RSV LRT in preterm infants (Griffin et al., 2020). Similarly, our data shows that increased levels of IgG1 in the coinfected group compared to the RSV group may be protective. The diminished RSV antibody response observed in this study may be attributed to the early euthanasia of the mice on days 7 and 4 post-RSV infection, which occurred before the expected antibody response could fully develop. The heightened antibody response in the coinfected groups may result from a synergistic effect stemming from the prior *P. murina*

antibody response combined with the early response to RSV. Consequently, the antibody response to *P. murina* may have primed the lung environment in the coinfected group towards a Th2 response, indicated by increased levels of IgG, IgG1, and Ig2b. Similarly, a previous study reported the immunomodulatory role of a helminth, *Trichinella spiralis,* on subsequent RSV infection (Chu et al., 2020). It was observed that the pre-existing *Trichinella spiralis* enhanced RSV-specific antibodies, which reduced the viral replication (Chu et al., 2020).

Pneumocystis jirovecii pneumonia is a major comorbidity factor in patients with advanced HIV disease and other immunodeficiencies as well as in malnourished children, which promotes simultaneous infection with other micro-organisms (Shann et al. (1986); Roths et al. (1993)). RAG1-deficient mice are deficient in T and B cells, making them more susceptible to severe infections, similar to immunocompromised individuals. In this study, we further coinfected RAG1-deficient mice with *P. murina* and RSV to see if there would be any differences in the clearance in an immunocompromised host. Similarly, *P. murina* reduced the RSV burden in the coinfected group, and the fungal burden was reduced in the coinfected group. Contrary to the mucus production associated with *P. murina*-infected WT mice, the mucus production in RAG1-deficient mice was not evident. The high RSV burden in the RSV control group was associated with elevated levels of IFN-β. While there were no significant differences between the coinfected group and the RSV group, the levels of IFN-β were elevated to a lesser extent. This may indicate that reduced RSV in the coinfected group is due to decreased viral replication, not the effects of an antiviral response caused by IFN-β. The pro-inflammatory cytokines IL-1β, TNF-α, and IL-12p70 were elevated in the *P. murina* and coinfected group. The reduced RSV burden in the coinfected group could be because the *P. murina* primed the lung pro-inflammatory response before the coinfection with RSV.

Plaque assays are used to quantify the load of infectious particles on a sample (Bae et al., 2003). In this study, a plaque assay was attempted to determine the virus concentration, but it was unsuccessful. This could be due to the degradation of the virus during the thawing. Plaques require a long incubation time to form, between 4 to 7 days; they may be damaged during this process (Kim et al., 2017). In contrast, qPCR offers a more rapid and reliable detection for quantifying the viral load, as the viral RNA is better preserved by immersion of the lung sample in Trizol immediately upon collection. With qPCR, we determined the viral burden in the lung samples.

Taken together, we see that both WT and RAG1-deficient mice demonstrate an increased ability to clear RSV when coinfected with *P. murina*. Immunocompetent individuals are often colonised with *P. jirovecii*. Consequently, the presence of *P. jirovecii* in the lungs of immunocompetent individuals may reduce the impact of RSV coinfection, as demonstrated by

the influence of *P. murina* on RSV coinfection in WT mice. Moreover, immunosuppressed individuals, who are typically susceptible to opportunistic infections, may also encounter milder effects from *P. jirovecii* or RSV when these pathogens coexist within the host, as demonstrated by the RAG1-deficient mice. The enhanced viral clearance observed in WT and RAG1-deficient mice may be attributed to the combined effects of increased mucus secretion, increased production of pro-inflammatory cytokines, or reduced viral replication. Additionally, the reduced RSV burden in WT mice could be attributable to the increased antibody response. Other experimental groups and time points, such as an uninfected group or the euthanasia of the *P. murina* at day 7 days post-infection, could have been beneficial in determining the immune status of the mice before RSV infection. Although establishing the baseline cytokine levels would have been informative, we could not justify the inclusion of a mock-infected group in our ethics protocol, as we were only interested in comparing relative cytokine levels between coinfected and RSV-only infected groups in this study. In addition to the cytokines analysed in this study, measuring the levels of Th2 and Th17 cytokines would have been beneficial to provide more insight into the effects of *P. murina* on RSV infection.

7. Limitations and Future Directions

In this study, we effectively evaluated the presence of Kex1 in mice, however, the polyclonal antiserum has not been applied to human samples. A future study should attempt to test the reactivity of Kex1 in human samples for the development of monoclonal antibodies and a lateral flow assay.

In addition to *P. murina* visualisation and mucus production, we also attempted to visualise the inflammatory response during *P. murina* and RSV coinfection through H&E. However, this was not successful. The tissue inflammatory response will be optimised and form part of my PhD project. Human respiratory syncytial virus does not naturally infect mice, exhibiting limited replication capabilities within this species. Consequently, higher doses of the virus are typically necessary for effective replication and pathology, complicating the evaluation of disease parameters beyond viral load. To address this limitation, our future research will use a more tractable murine model, the Pneumonia Virus of Mice (PVM) developed by Benjamin Dewals (University of Liège, Belgium). As part of a collaborative project and my doctoral studies (recently funded by the National Research Foundation), I will visit Liege and receive training on the PVM model. This will include training in *in vivo* imaging using the PVM-luciferase reporter virus, which will track the virus and cell interactions during acute infections in mice. We will include the analysis of the tissue-specific inflammatory response through H&E staining during coinfection and determine the impact of *P. murina* exposure on immunohistopathology.

We will also scrutinise the cell type and associated cellular responses using flow cytometry in a proof-of-concept study by Dewals, we established that *P. murina* can reduce viral replication in mice coinfected with PVM-luciferase and reduce the weight loss associated with disease severity in a low-dose PVM infection model. We hypothesise that *P. murina* binds Type I pneumocytes, also required for viral replication, and prevents viral pneumonia and will expand these studies supported by the National Research Foundation.

8. Conclusion

The detection of Kex1 in pulmonary tissues as well as in non-invasive specimens like urine and serum makes it a promising tool for the rapid and non-invasive diagnosis of PCP through a lateral flow assay.

Furthermore, our study supports the notion that coinfections have the potential to be antagonistic towards each other. *Pneumocystis* may reduce the pathology associated with viral pneumonia, which could have the potential to provide therapeutic targets for childhood pneumonia. Additionally, understanding the immune response during coinfections could offer potential therapeutic avenues for addressing childhood pneumonia. Host-directed therapies potentially discovered through this type of work can be effective for both people living with HIV with normal CD4 T cell count and immunocompromised people.

References

2019. Causes of severe pneumonia requiring hospital admission in children without HIV infection from Africa and Asia: the PERCH multi-country case-control study. *Lancet,* 394**,** 757-779.

AGAC, A., KOLBE, S. M., LUDLOW, M., OSTERHAUS, A. D., MEINEKE, R. & RIMMELZWAAN, G. F. 2023. Host responses to respiratory syncytial virus infection. *Viruses,* 15**,** 1999.

AGRAWAL, B. 2019. Heterologous Immunity: Role in Natural and Vaccine-Induced Resistance to Infections. *Front Immunol,* 10**,** 2631.

ALBARBAR, B. 2024. The Importance of IgM and IgG Antibodies Testing in Infectious Diseases. *Libyan Medical Journal***,** 84-89.

ALIOUAT-DENIS, C.-M., CHABÉ, M., DEMANCHE, C., VISCOGLIOSI, E., GUILLOT, J., DELHAES, L. & DEI-CAS, E. 2008. Pneumocystis species, co-evolution and pathogenic power. *Infection, Genetics and Evolution,* 8**,** 708-726.

ALIOUAT-DENIS, C.-M., MARTINEZ, A., ALIOUAT, E. M., POTTIER, M., GANTOIS, N. & DEI-CAS, E. 2009. The Pneumocystis life cycle. *Memorias do Instituto Oswaldo Cruz,* 104**,** 419-426.

APOSTOLOPOULOU, A. & FISHMAN, J. A. 2022. The pathogenesis and diagnosis of Pneumocystis jiroveci pneumonia. *Journal of Fungi,* 8**,** 1167.

ARTS, R. J., MOORLAG, S. J., NOVAKOVIC, B., LI, Y., WANG, S.-Y., OOSTING, M., KUMAR, V., XAVIER, R. J., WIJMENGA, C. & JOOSTEN, L. A. 2018. BCG vaccination protects against experimental viral infection in humans through the induction of cytokines associated with trained immunity. *Cell host & microbe,* 23**,** 89-100. e5.

BAE, H.-G., NITSCHE, A., TEICHMANN, A., BIEL, S. S. & NIEDRIG, M. 2003. Detection of yellow fever virus: a comparison of quantitative real-time PCR and plaque assay. *Journal of Virological Methods,* 110**,** 185-191.

BAKALETZ, L. O. 2017. Viral–bacterial co-infections in the respiratory tract. *Current opinion in microbiology,* 35**,** 30-35.

BATEMAN, M., OLADELE, R. & KOLLS, J. K. 2020. Diagnosing Pneumocystis jirovecii pneumonia: A review of current methods and novel approaches. *Med Mycol,* 58**,** 1015-1028.

BATTLES, M. B. & MCLELLAN, J. S. 2019. Respiratory syncytial virus entry and how to block it. *Nature Reviews Microbiology,* 17**,** 233-245.

BECK, J. M. & CUSHION, M. T. 2009. Pneumocystis workshop: 10th anniversary summary. *Eukaryot Cell,* 8**,** 446-60.

BECK, J. M., WARNOCK, M. L., CURTIS, J. L., SNIEZEK, M. J., ARRAJ-PEFFER, S. M., KALTREIDER, H. B. & SHELLITO, J. E. 1991. Inflammatory responses to Pneumocystis carinii in mice selectively depleted of helper T lymphocytes. *Am J Respir Cell Mol Biol,* 5**,** 186-97.

BELLO-IRIZARRY, S. N., WANG, J., OLSEN, K., GIGLIOTTI, F. & WRIGHT, T. W. 2012. The Alveolar Epithelial Cell Chemokine Response to Pneumocystis Requires Adaptor Molecule MyD88 and Interleukin-1 Receptor but Not Toll-Like Receptor 2 or 4. *Infection and Immunity,* 80**,** 3912-3920.

BEM, R. A., DOMACHOWSKE, J. B. & ROSENBERG, H. F. 2011. Animal models of human respiratory syncytial virus disease. *American Journal of Physiology-Lung Cellular and Molecular Physiology,* 301**,** L148-L156.

BHAGWAT, S. P., GIGLIOTTI, F., XU, H. & WRIGHT, T. W. 2006. Contribution of T cell subsets to the pathophysiology of Pneumocystis-related immunorestitution disease. *American Journal of Physiology-Lung Cellular and Molecular Physiology,* 291**,** L1256-L1266.

BONGOMIN, F., EKENG, B. E., KIBONE, W., NSENGA, L., OLUM, R., ITAM-EYO, A., KUATE, M. P. N., PEBOLO, F. P., DAVIES, A. A., MANGA, M., OCANSEY, B., KWIZERA, R. & BALUKU, J. B. 2022. Invasive Fungal Diseases in Africa: A Critical Literature Review. *Journal of Fungi,* 8**,** 1236.

BONGOMIN, F., GAGO, S., OLADELE, R. O. & DENNING, D. W. 2017. Global and Multi-National Prevalence of Fungal Diseases-Estimate Precision. *J Fungi (Basel),* 3.

BORCHERS, A. T., CHANG, C., GERSHWIN, M. E. & GERSHWIN, L. J. 2013. Respiratory syncytial virus—a comprehensive review. *Clinical reviews in allergy & immunology,* 45**,** 331-379.

BOSTICARDO, M., PALA, F. & NOTARANGELO, L. D. 2021. RAG deficiencies: Recent advances in disease pathogenesis and novel therapeutic approaches. *Eur J Immunol,* 51**,** 1028-1038.

BROGDEN, K. A., GUTHMILLER, J. M. & TAYLOR, C. E. 2005. Human polymicrobial infections. *The Lancet,* 365**,** 253-255.

BROWN, G. D., DENNING, D. W., GOW, N. A., LEVITZ, S. M., NETEA, M. G. & WHITE, T. C. 2012. Hidden killers: human fungal infections. *Science translational medicine,* 4**,** 165rv13-165rv13.

CABALLERO, M. T., SERRA, M. E., ACOSTA, P. L., MARZEC, J., GIBBONS, L., SALIM, M., RODRIGUEZ, A., REYNALDI, A., GARCIA, A. & BADO, D. 2015. TLR4 genotype and environmental LPS mediate RSV bronchiolitis through Th2 polarization. *The Journal of clinical investigation,* 125**,** 571-582.

CANNON, M., OPENSHAW, P. & ASKONAS, B. 1988. Cytotoxic T cells clear virus but augment lung pathology in mice infected with respiratory syncytial virus. *The Journal of experimental medicine,* 168**,** 1163-1168.

CARMONA, E. M. & LIMPER, A. H. 2011. Update on the diagnosis and treatment of Pneumocystis pneumonia. *Therapeutic Advances in Respiratory Disease,* 5**,** 41-59.

CHARPENTIER, E., MÉNARD, S., MARQUES, C., BERRY, A. & IRIART, X. 2021. Immune Response in Pneumocystis Infections According to the Host Immune System Status. *J Fungi (Basel),* 7.

CHEN, W., HAVELL, E., GIGLIOTTI, F. & HARMSEN, A. 1993. Interleukin-6 production in a murine model of Pneumocystis carinii pneumonia: relation to resistance and inflammatory response. *Infection and immunity,* 61**,** 97-102.

CHOE, P. G., KANG, Y. M., KIM, G., PARK, W. B., PARK, S. W., KIM, H. B., OH, M.-D., KIM, E. C. & KIM, N. J. 2014. Diagnostic value of direct fluorescence antibody staining for detecting Pneumocystis jirovecii in expectorated sputum from patients with HIV infection. *Medical Mycology,* 52**,** 326-330.

CHU, K. B., LEE, H. A., KANG, H. J., MOON, E. K. & QUAN, F. S. 2020. Preliminary Trichinella spiralis Infection Ameliorates Subsequent RSV Infection-Induced Inflammatory Response. *Cells,* 9.

CHURISO, G., HUSEN, G., BULBULA, D. & ABEBE, L. 2022. Immunity cell responses to RSV and the role of antiviral inhibitors: a systematic review. *Infection and drug resistance***,** 7413-7430.

COBOS JIMÉNEZ, V., RABACAL, W., RAYENS, E. & NORRIS, K. A. 2019. Immunization with Pneumocystis recombinant KEX1 induces robust and durable humoral responses in immunocompromised non-human primates. *Hum Vaccin Immunother,* 15**,** 2075-2080.

COHN, L., HOMER, R. J., MACLEOD, H., MOHRS, M., BROMBACHER, F. & BOTTOMLY, K. 1999. Th2-Induced Airway Mucus Production Is Dependent on IL-4Rα, But Not on Eosinophils1. *The Journal of Immunology,* 162**,** 6178-6183.

COLLINS, P. L. & GRAHAM, B. S. 2008. Viral and host factors in human respiratory syncytial virus pathogenesis. *Journal of virology,* 82**,** 2040-2055.

DECKMAN, J. M., KURKJIAN, C. J., MCGILLIS, J. P., CORY, T. J., BIRKET, S. E., SCHUTZMAN, L. M., MURPHY, B. S., GARVY, B. A. & FEOLA, D. J. 2017. Pneumocystis infection alters the activation state of pulmonary macrophages. *Immunobiology,* 222**,** 188-197.

DEL CORPO, O., BUTLER-LAPORTE, G., SHEPPARD, D. C., CHENG, M. P., MCDONALD, E. G. & LEE, T. C. 2020. Diagnostic accuracy of serum (1-3)-β-D-glucan for Pneumocystis jirovecii pneumonia: a systematic review and meta-analysis. *Clin Microbiol Infect,* 26**,** 1137-1143.

DENNING, D. W. 2024. Global incidence and mortality of severe fungal disease. *Lancet Infect Dis,* 24**,** e428-e438.

DING, K., SHIBUI, A., WANG, Y., TAKAMOTO, M., MATSUGUCHI, T. & SUGANE, K. 2005. Impaired recognition by Toll-like receptor 4 is responsible for exacerbated murine Pneumocystis pneumonia. *Microbes and infection,* 7**,** 195-203.

DJAWE, K., HUANG, L., DALY, K. R., LEVIN, L., KOCH, J., SCHWARTZMAN, A., FONG, S., ROTH, B., SUBRAMANIAN, A., GRIECO, K., JARLSBERG, L. & WALZER, P. D. 2010. Serum antibody levels to the Pneumocystis jirovecii major surface glycoprotein in the diagnosis of P. jirovecii pneumonia in HIV+ patients. *PLoS One,* 5**,** e14259.

DOMACHOWSKE, J. B., BONVILLE, C. A., DYER, K. D., EASTON, A. J. & ROSENBERG, H. F. 2000. Pulmonary Eosinophilia and Production of MIP-1α Are Prominent Responses to Infection with Pneumonia Virus of Mice. *Cellular Immunology,* 200**,** 98-104.

DOMACHOWSKE, J. B., BONVILLE, C. A., EASTON, A. J. & ROSENBERG, H. F. 2002. Differential Expression of Proinflammatory Cytokine Genes In Vivo in Response to Pathogenic and Nonpathogenic Pneumovirus Infections. *The Journal of Infectious Diseases,* 186**,** 8-14.

DOMACHOWSKE, J. B. & ROSENBERG, H. F. 1999. Respiratory syncytial virus infection: immune response, immunopathogenesis, and treatment. *Clin Microbiol Rev,* 12**,** 298-309.

DUFAUD, C., RIVERA, J., ROHATGI, S. & PIROFSKI, L. A. 2018. Naïve B cells reduce fungal dissemination in Cryptococcus neoformans infected Rag1(-/-) mice. *Virulence,* 9**,** 173-184.

DURBIN, J. E., JOHNSON, T. R., DURBIN, R. K., MERTZ, S. E., MOROTTI, R. A., PEEBLES, R. S. & GRAHAM, B. S. 2002. The Role of IFN in Respiratory Syncytial Virus Pathogenesis. *The Journal of Immunology,* 168**,** 2944-2952.

DYER, K. D., GARCIA-CRESPO, K. E., GLINEUR, S., DOMACHOWSKE, J. B. & ROSENBERG, H. F. 2012. The pneumonia virus of mice (PVM) model of acute respiratory infection. *Viruses,* 4**,** 3494-3510.

EDDENS, T. & KOLLS, J. K. Pathological and protective immunity to Pneumocystis infection. Seminars in immunopathology, 2015. Springer, 153-162.

ESTEVES, F., CALÉ, S. S., BADURA, R., DE BOER, M. G., MALTEZ, F., CALDERÓN, E. J., VAN DER REIJDEN, T. J., MÁRQUEZ-MARTÍN, E., ANTUNES, F. & MATOS, O. 2015. Diagnosis of Pneumocystis pneumonia: evaluation of four serologic biomarkers. *Clin Microbiol Infect,* 21**,** 379.e1-10.

ESTEVES, F., LEE, C. H., DE SOUSA, B., BADURA, R., SERINGA, M., FERNANDES, C., GASPAR, J. F., ANTUNES, F. & MATOS, O. 2014. (1–3)-Beta-D-glucan in association with lactate dehydrogenase as biomarkers of Pneumocystis pneumonia (PcP) in HIV-infected patients. *European Journal of Clinical Microbiology & Infectious Diseases,* 33**,** 1173-1180.

FREITAS, G., SILVA, D., YOKOSAWA, J., PAULA, N., COSTA, L., CARNEIRO, B., RIBEIRO, L., OLIVEIRA, T., MINEO, J. & QUEIROZ, D. 2011. Antibody response and avidity of respiratory syncytial virus-specific total IgG, IgG1, and IgG3 in young children. *Journal of medical virology,* 83**,** 1826-1833.

GALLOUX, M., RISSO-BALLESTER, J., RICHARD, C. A., FIX, J., RAMEIX-WELTI, M. A. & ELÉOUËT, J. F. 2020. Minimal Elements Required for the Formation of Respiratory Syncytial Virus Cytoplasmic Inclusion Bodies In Vivo and In Vitro. *mBio,* 11.

GARVEY, T. L., DYER, K. D., ELLIS, J. A., BONVILLE, C. A., FOSTER, B., PRUSSIN, C., EASTON, A. J., DOMACHOWSKE, J. B. & ROSENBERG, H. F. 2005. Inflammatory Responses to Pneumovirus Infection in IFN-αβR Gene-Deleted Mice1. *The Journal of Immunology,* 175**,** 4735-4744.

GIGLIOTTI, F., HAIDARIS, C. G., WRIGHT, T. W. & HARMSEN, A. G. 2002. Passive Intranasal Monoclonal Antibody Prophylaxis against Murine Pneumocystis carinii Pneumonia. *Infection and Immunity,* 70**,** 1069-1074.

GIGLIOTTI, F., LIMPER, A. H. & WRIGHT, T. 2014. Pneumocystis. *Cold Spring Harb Perspect Med,* 4**,** a019828.

GINGERICH, A. D., NORRIS, K. A. & MOUSA, J. J. 2021. Pneumocystis pneumonia: immunity, vaccines, and treatments. *Pathogens,* 10**,** 236.

GINGO, M. R., LUCHT, L., DALY, K. R., DJAWE, K., PALELLA, F. J., ABRAHAM, A. G., BREAM, J. H., WITT, M. D., KINGSLEY, L. A. & NORRIS, K. A. 2011. Serologic responses to pneumocystis proteins in HIV patients with and without Pneumocystis jirovecii pneumonia. *JAIDS Journal of Acquired Immune Deficiency Syndromes,* 57**,** 190-196.

GORITZKA, M., DURANT, L. R., PEREIRA, C., SALEK-ARDAKANI, S., OPENSHAW, P. J. M. & JOHANSSON, C. 2014. Alpha/Beta Interferon Receptor Signaling Amplifies Early Proinflammatory Cytokine

Production in the Lung during Respiratory Syncytial Virus Infection. *Journal of Virology,* 88**,** 6128-6136.

GRIFFIN, M. P., YUAN, Y., TAKAS, T., DOMACHOWSKE, J. B., MADHI, S. A., MANZONI, P., SIMÕES, E. A., ESSER, M. T., KHAN, A. A. & DUBOVSKY, F. 2020. Single-dose nirsevimab for prevention of RSV in preterm infants. *New England Journal of Medicine,* 383**,** 415-425.

GRIFFITHS, E. C., PEDERSEN, A. B., FENTON, A. & PETCHEY, O. L. 2011. The nature and consequences of coinfection in humans. *Journal of Infection,* 63**,** 200-206.

GRØNSETH, S., ROGNE, T., HANNULA, R., ÅSVOLD, B. O., AFSET, J. E. & DAMÅS, J. K. 2021. Semiquantitative Real-Time PCR to Distinguish Pneumocystis Pneumonia from Colonization in a Heterogeneous Population of HIV-Negative Immunocompromised Patients. *Microbiology Spectrum,* 9.

GUEGAN, H. & ROBERT-GANGNEUX, F. 2019. Molecular diagnosis of Pneumocystis pneumonia in immunocompromised patients. *Curr Opin Infect Dis,* 32**,** 314-321.

HAMILTON, R. G. 1987. Human IgG subclass measurements in the clinical laboratory. *Clinical Chemistry,* 33**,** 1707-1725.

HÄNSEL, L., SCHUMACHER, J., DENIS, B., HAMANE, S., CORNELY, O. A. & KOEHLER, P. 2023. How to diagnose and treat a non-HIV patient with Pneumocystis jirovecii pneumonia (PCP)? *Clinical Microbiology and Infection*.

HARMSEN, A. G. & STANKIEWICZ, M. 1990. Requirement for CD4+ cells in resistance to Pneumocystis carinii pneumonia in mice. *Journal of Experimental Medicine,* 172**,** 937-945.

HAYNES, L. M., MOORE, D. D., KURT-JONES, E. A., FINBERG, R. W., ANDERSON, L. J. & TRIPP, R. A. 2001. Involvement of Toll-Like Receptor 4 in Innate Immunity to Respiratory Syncytial Virus. *Journal of Virology,* 75**,** 10730-10737.

HENNUS, M. P., JANSSEN, R., PENNINGS, J. L. A., HODEMAEKERS, H. M., KRUIJSEN, D., JANSEN, N. J., MEYAARD, L., VAN VUGHT, A. J. & BONT, L. J. 2012. Host response to mechanical ventilation for viral respiratory tract infection. *European Respiratory Journal,* 40**,** 1508-1515.

HORNSLETH, A., BECH-THOMSEN, N. & FRIIS, B. 1985. Detection by ELISA of IgG-subclass-specific antibodies in primary respiratory syncytial (RS) virus infections. *Journal of medical virology,* 16**,** 321-328.

HORNSLETH, A., KLUG, B., NIR, M., JOHANSEN, J., HANSEN, K. S., CHRISTENSEN, L. S. & LARSEN, L. B. 1998. Severity of respiratory syncytial virus disease related to type and genotype of virus and to cytokine values in nasopharyngeal secretions. *The Pediatric infectious disease journal,* 17**,** 1114-1121.

HOVING, J. C. & KOLLS, J. K. 2017. New advances in understanding the host immune response to Pneumocystis. *Curr Opin Microbiol,* 40**,** 65-71.

HOVING, J. C., MUNYONHO, F. T. & KOLLS, J. K. 2023. Genetic Mouse Models of Pneumocystis Pneumonia. *Antifungal Immunity: Methods and Protocols.* Springer.

HUANG, L., CATTAMANCHI, A., DAVIS, J. L., BOON, S. D., KOVACS, J., MESHNICK, S., MILLER, R. F., WALZER, P. D., WORODRIA, W. & MASUR, H. 2011. HIV-associated Pneumocystis pneumonia. *Proceedings of the American Thoracic Society,* 8**,** 294-300.

IRIART, X., WITKOWSKI, B., COURTAIS, C., ABBES, S., TKACZUK, J., COURTADE, M., CASSAING, S., FILLAUX, J., BLANCHER, A., MAGNAVAL, J. F., PIPY, B. & BERRY, A. 2010. Cellular and cytokine changes in the alveolar environment among immunocompromised patients during Pneumocystis jirovecii infection. *Med Mycol,* 48**,** 1075-87.

ISLAM, N., IRFAN, M., ZAHOOR, A. F., SYED, H. K., SHAH, S., SHAH, M. A., SYED, M. A. & RAZA, S. A. 2023. Pneumocystis Carnii Pneumonia Infections: Disease, Diagnosis, and Treatment Options. *Infectious Diseases Drug Delivery Systems.* Springer.

ITURRA, P. A., ROJAS, D. A., PÉREZ, F. J., MÉNDEZ, A., PONCE, C. A., BONILLA, P., BUSTAMANTE, R., RODRÍGUEZ, H., BELTRÁN, C. J. & VARGAS, S. L. 2018. Progression of type 2 helper T Cell–type inflammation and airway remodeling in a rodent model of naturally acquired subclinical primary pneumocystis infection. *The American Journal of Pathology,* 188**,** 417-431.

JAFRI, H. S., CHÁVEZ-BUENO, S., MEJÍAS, A., GÓMEZ, A. M., RÍOS, A. M., NASSI, S. S., YUSUF, M., KAPUR, P., HARDY, R. D., HATFIELD, J., ROGERS, B. B., KRISHER, K. & RAMILO, O. 2004. Respiratory Syncytial Virus Induces Pneumonia, Cytokine Response, Airway Obstruction, and Chronic Inflammatory Infiltrates Associated with Long-Term Airway Hyperresponsiveness in Mice. *The Journal of Infectious Diseases,* 189**,** 1856-1865.

JHA, A., JARVIS, H., FRASER, C. & OPENSHAW, P. 2016. Respiratory syncytial virus. *SARS, MERS and other viral lung infections*.

JOFFRION, T. M. & CUSHION, M. T. 2010. Sterol biosynthesis and sterol uptake in the fungal pathogen Pneumocystis carinii. *FEMS microbiology letters,* 311**,** 1-9.

KALER, J., HUSSAIN, A., PATEL, K., HERNANDEZ, T. & RAY, S. 2023. Respiratory Syncytial Virus: A Comprehensive Review of Transmission, Pathophysiology, and Manifestation. *Cureus,* 15.

KAWAI, T. & AKIRA, S. TLR signaling. Seminars in immunology, 2007. Elsevier, 24-32.

KELLY, M. N. & SHELLITO, J. E. 2010. Current understanding of Pneumocystis immunology. *Future Microbiol,* 5**,** 43-65.

KIM, K. S., KIM, A. R., PIAO, Y., LEE, J. H. & QUAN, F. S. 2017. A rapid, simple, and accurate plaque assay for human respiratory syncytial virus (HRSV). *J Immunol Methods,* 446**,** 15-20.

KIM, T. H. & LEE, H. K. 2014. Innate immune recognition of respiratory syncytial virus infection. *BMB reports,* 47**,** 184.

KINNEAR, E., LAMBERT, L., MCDONALD, J. U., CHEESEMAN, H. M., CAPRONI, L. J. & TREGONING, J. S. 2018. Airway T cells protect against RSV infection in the absence of antibody. *Mucosal Immunology,* 11**,** 249-256.

KLING, H. M., SHIPLEY, T. W., PATIL, S. P., KRISTOFF, J., BRYAN, M., MONTELARO, R. C., MORRIS, A. & NORRIS, K. A. 2010. Relationship of Pneumocystis jiroveci humoral immunity to prevention of colonization and chronic obstructive pulmonary disease in a primate model of HIV infection. *Infection and immunity,* 78**,** 4320-4330.

KOLLS, J. K., HABETZ, S., SHEAN, M. K., VAZQUEZ, C., BROWN, J. A., LEI, D., SCHWARZENBERGER, P., YE, P., NELSON, S. & SUMMER, W. R. 1999. IFN-γ and CD8+ T cells restore host defenses against Pneumocystis carinii in mice depleted of CD4+ T cells. *The Journal of Immunology,* 162**,** 2890-2894.

KUTTY, G., DAVIS, A. S., FERREYRA, G. A., QIU, J., HUANG, D. W., SASSI, M., BISHOP, L., HANDLEY, G., SHERMAN, B. & LEMPICKI, R. 2016. β-glucans are masked but contribute to pulmonary inflammation during Pneumocystis pneumonia. *The Journal of Infectious Diseases,* 214**,** 782-791.

KUTTY, G. & KOVACS, J. A. 2003. A single-copy gene encodes Kex1, a serine endoprotease of Pneumocystis jiroveci. *Infect Immun,* 71**,** 571-4.

LARSEN, H. H., HUANG, L., KOVACS, J. A., CROTHERS, K., SILCOTT, V. A., MORRIS, A., TURNER, J. R., BEARD, C. B., MASUR, H. & FISHER, S. H. 2004. A Prospective, Blinded Study of Quantitative Touch-Down Polymerase Chain Reaction Using Oral-Wash Samples for Diagnosis of Pneumocystis Pneumonia in HIV-Infected Patients. *The Journal of Infectious Diseases,* 189**,** 1679-1683.

LEE, L. H., GIGLIOTTI, F., WRIGHT, T. W., SIMPSON-HAIDARIS, P. J., WEINBERG, G. A. & HAIDARIS, C. G. 2000. Molecular characterization of KEX1, a kexin-like protease in mouse Pneumocystis carinii. *Gene,* 242**,** 141-150.

LIMPER, A. H., HOYTE, J. S. & STANDING, J. E. 1997. The role of alveolar macrophages in Pneumocystis carinii degradation and clearance from the lung. *The Journal of clinical investigation,* 99**,** 2110-2117.

LIPSCHIK, G. Y., ANDRAWIS, V., OGNIBENE, F., KOVACS, J., GILL, V., NELSON, N., LUNDGREN, J. & NIELSEN, J. 1992. Improved diagnosis of Pneumocystis carinii infection by polymerase chain reaction on induced sputum and blood. *The Lancet,* 340**,** 203-206.

LUND, F. E., HOLLIFIELD, M., SCHUER, K., LINES, J. L., RANDALL, T. D. & GARVY, B. A. 2006. B cells are required for generation of protective effector and memory CD4 cells in response to Pneumocystis lung infection. *J Immunol,* 176**,** 6147-54.

MA, L., CISSÉ, O. H. & KOVACS, J. A. 2018. A Molecular Window into the Biology and Epidemiology of Pneumocystis spp. *Clin Microbiol Rev,* 31.

MALDONADO, S. & FITZGERALD-BOCARSLY, P. 2017. Antifungal Activity of Plasmacytoid Dendritic Cells and the Impact of Chronic HIV Infection. *Front Immunol,* 8**,** 1705.

MARTIN, W. J. & PASULA, R. 2000. Role of alveolar macrophages in host defense against Pneumocystis carinii. *American Journal of Respiratory Cell and Molecular Biology,* 23**,** 434-435.

MCARDLE, A. J., TURKOVA, A. & CUNNINGTON, A. J. 2018. When do co-infections matter? *Current opinion in infectious diseases,* 31**,** 209.

MCMULLAN, B., KIM, H. Y., ALASTRUEY-IZQUIERDO, A., TACCONELLI, E., DAO, A., OLADELE, R., TANTI, D., GOVENDER, N. P., SHIN, J.-H. & HEIM, J. 2024. Features and global impact of invasive fungal infections caused by Pneumocystis jirovecii: A systematic review to inform the World Health Organization fungal priority pathogens list. *Medical Mycology,* 62**,** myae038.

MCNAB, F., MAYER-BARBER, K., SHER, A., WACK, A. & O'GARRA, A. 2015. Type I interferons in infectious disease. *Nature Reviews Immunology,* 15**,** 87-103.

MCNAMARA, P., FONCECA, A., HOWARTH, D., CORREIA, J., SLUPSKY, J., TRINICK, R., AL TURAIKI, W., SMYTH, R. & FLANAGAN, B. 2013. Respiratory syncytial virus infection of airway epithelial cells, in vivo and in vitro, supports pulmonary antibody responses by inducing expression of the B cell differentiation factor BAFF. *Thorax,* 68**,** 76-81.

MOORLAG, S., RÖRING, R. J., JOOSTEN, L. A. B. & NETEA, M. G. 2018. The role of the interleukin-1 family in trained immunity. *Immunol Rev,* 281**,** 28-39.

MORRIS, A. & NORRIS, K. A. 2012. Colonization by Pneumocystis jirovecii and its role in disease. *Clinical microbiology reviews,* 25**,** 297-317.

MURAWSKI, M. R., BOWEN, G. N., CERNY, A. M., ANDERSON, L. J., HAYNES, L. M., TRIPP, R. A., KURT-JONES, E. A. & FINBERG, R. W. 2009. Respiratory Syncytial Virus Activates Innate Immunity through Toll-Like Receptor 2. *Journal of Virology,* 83**,** 1492-1500.

NANDAKUMAR, V., HEBRINK, D., JENSON, P., KOTTOM, T. & LIMPER, A. H. 2017. Differential Macrophage Polarization from Pneumocystis in Immunocompetent and Immunosuppressed Hosts: Potential Adjunctive Therapy during Pneumonia. *Infection and Immunity,* 85**,** 10.1128/iai.00939-16.

NELSON, M. P., CHRISTMANN, B. S., WERNER, J. L., METZ, A. E., TREVOR, J. L., LOWELL, C. A. & STEELE, C. 2011. IL-33 and M2a Alveolar Macrophages Promote Lung Defense against the Atypical Fungal Pathogen Pneumocystis murina. *The Journal of Immunology,* 186**,** 2372-2381.

NETEA, M. G., DOMÍNGUEZ-ANDRÉS, J., BARREIRO, L. B., CHAVAKIS, T., DIVANGAHI, M., FUCHS, E., JOOSTEN, L. A. B., VAN DER MEER, J. W. M., MHLANGA, M. M., MULDER, W. J. M., RIKSEN, N. P., SCHLITZER, A., SCHULTZE, J. L., STABELL BENN, C., SUN, J. C., XAVIER, R. J. & LATZ, E. 2020. Defining trained immunity and its role in health and disease. *Nature Reviews Immunology,* 20**,** 375-388.

NG, V. L., YAJKO, D. M. & HADLEY, W. K. 1997. Extrapulmonary pneumocystosis. *Clinical Microbiology Reviews,* 10**,** 401-418.

OTIENO-ODHIAMBO, P., WASSERMAN, S. & HOVING, J. C. 2019. The Contribution of Host Cells to Pneumocystis Immunity: An Update. *Pathogens,* 8**,** 52.

PARSONS, E. L., KIM, J. S. & MALLOY, A. M. 2024. Development of innate and adaptive immunity to RSV in young children. *Cellular Immunology***,** 104824.

PERCOPO, C. M., MA, M., BRENNER, T. A., KRUMHOLZ, J. O., BREAK, T. J., LAKY, K. & ROSENBERG, H. F. 2019. Critical Adverse Impact of IL-6 in Acute Pneumovirus Infection. *J Immunol,* 202**,** 871-882.

PERCOPO, C. M., MA, M. & ROSENBERG, H. F. 2017. Administration of immunobiotic Lactobacillus plantarum delays but does not prevent lethal pneumovirus infection in Rag1(-/-) mice. *J Leukoc Biol,* 102**,** 905-913.

PIFER, L. L., HUGHES, W. T., STAGNO, S. & WOODS, D. 1978. Pneumocystis carinii infection: evidence for high prevalence in normal and immunosuppressed children. *Pediatrics,* 61**,** 35-41.

POP, S. M., KOLLS, J. K. & STEELE, C. 2006. Pneumocystis: Immune recognition and evasion. *The International Journal of Biochemistry & Cell Biology,* 38**,** 17-22.

PRIBUL, P. K., HARKER, J., WANG, B., WANG, H., TREGONING, J. S., SCHWARZE, J. R. & OPENSHAW, P. J. 2008. Alveolar macrophages are a major determinant of early responses to viral lung infection but do not influence subsequent disease development. *Journal of virology,* 82**,** 4441-4448.

PUNGAN, D., FAN, J., DAI, G., KHATUN, M. S., DIETRICH, M. L., ZWEZDARYK, K. J., ROBINSON, J. E., LANDRY, S. J. & KOLLS, J. K. 2023. Novel Pneumocystis Antigens for Seroprevalence Studies. *Journal of Fungi,* 9**,** 602.

RAPAKA, R. R., RICKS, D. M., ALCORN, J. F., CHEN, K., KHADER, S. A., ZHENG, M., PLEVY, S., BENGTÉN, E. & KOLLS, J. K. 2010. Conserved natural IgM antibodies mediate innate and adaptive immunity against the opportunistic fungus Pneumocystis murina. *Journal of Experimental Medicine,* 207**,** 2907-2919.

REED, J. L., WELLIVER, T. P., SIMS, G. P., MCKINNEY, L., VELOZO, L., AVENDANO, L., HINTZ, K., LUMA, J., COYLE, A. J. & WELLIVER, S., ROBERT C. 2009. Innate Immune Signals Modulate Antiviral and Polyreactive Antibody Responses during Severe Respiratory Syncytial Virus Infection. *The Journal of Infectious Diseases,* 199**,** 1128-1138.

ROTHS, J. B., SMITH, A. L. & SIDMAN, C. L. 1993. Lethal exacerbation of Pneumocystis carinii pneumonia in severe combined immunodeficiency mice after infection by pneumonia virus of mice. *The Journal of experimental medicine,* 177**,** 1193-1198.

RUAN, S., MCKINLEY, L., ZHENG, M., RUDNER, X., D'SOUZA, A., KOLLS, J. K. & SHELLITO, J. E. 2008. Interleukin-12 and Host Defense against Murine Pneumocystis Pneumonia. *Infection and Immunity,* 76**,** 2130-2137.

RUCKWARDT, T. J., MORABITO, K. M. & GRAHAM, B. S. 2019. Immunological lessons from respiratory syncytial virus vaccine development. *Immunity,* 51**,** 429-442.

RUDD, B. D., SMIT, J. J., FLAVELL, R. A., ALEXOPOULOU, L., SCHALLER, M. A., GRUBER, A., BERLIN, A. A. & LUKACS, N. W. 2006. Deletion of TLR3 Alters the Pulmonary Immune Environment and Mucus Production during Respiratory Syncytial Virus Infection. *The Journal of Immunology,* 176**,** 1937-1942.

RUDNER, X. L., HAPPEL, K. I., YOUNG, E. A. & SHELLITO, J. E. 2007. Interleukin-23 (IL-23)-IL-17 cytokine axis in murine Pneumocystis carinii infection. *Infection and immunity,* 75**,** 3055-3061.

RUSSELL, C. D., UNGER, S. A., WALTON, M. & SCHWARZE, J. 2017. The human immune response to respiratory syncytial virus infection. *Clinical microbiology reviews,* 30**,** 481-502.

SALAZAR, F., BIGNELL, E., BROWN, G. D., COOK, P. C. & WARRIS, A. 2022. Pathogenesis of Respiratory Viral and Fungal Coinfections. *Clinical Microbiology Reviews,* 35**,** e00094-21.

SALIMI, V., VIEGAS, M., TRENTO, A., AGOTI, C. N., ANDERSON, L. J., AVADHANULA, V., BAHL, J., BONT, L., BRISTER, J. R. & CANE, P. A. 2021. Proposal for human respiratory syncytial virus nomenclature below the species level. *Emerging infectious diseases,* 27.

SATO, K., YANG, X.-L., YUDATE, T., CHUNG, J.-S., WU, J., LUBY-PHELPS, K., KIMBERLY, R. P., UNDERHILL, D., CRUZ, P. D. & ARIIZUMI, K. 2006. Dectin-2 is a pattern recognition receptor for fungi that couples with the Fc receptor γ chain to induce innate immune responses. *Journal of Biological Chemistry,* 281**,** 38854-38866.

SCHAFFZIN, J. K., SUNKIN, S. M. & STRINGER, J. R. 1999. A new family of Pneumocystis carinii genes related to those encoding the major surface glycoprotein. *Curr Genet,* 35**,** 134-43.

SCHMIDT, M. E. & VARGA, S. M. 2017. Modulation of the host immune response by respiratory syncytial virus proteins. *J Microbiol,* 55**,** 161-171.
SCHMIDT, M. E. & VARGA, S. M. 2018. The CD8 T cell response to respiratory virus infections. *Frontiers in immunology,* 9**,** 678.
SHANN, F., WALTERS, S., PIFER, L. L., GRAHAM, D. M., JACK, I., UREN, E., BIRCH, D. & STALLMAN, N. D. 1986. Pneumonia associated with infection with pneumocystis, respiratory syncytial virus, chlamydia, mycoplasma, and cytomegalovirus in children in Papua New Guinea. *Br Med J (Clin Res Ed),* 292**,** 314-317.
SHELLITO, J. E., TATE, C., RUAN, S. & ROLLS, J. 2000. Murine CD4+ T Lymphocyte Subsets and Host Defense against Pneumocystis carinii. *The Journal of Infectious Diseases,* 181**,** 2011-2017.
SHI, T., MCALLISTER, D. A., O'BRIEN, K. L., SIMOES, E. A., MADHI, S. A., GESSNER, B. D., POLACK, F. P., BALSELLS, E., ACACIO, S. & AGUAYO, C. 2017. Global, regional, and national disease burden estimates of acute lower respiratory infections due to respiratory syncytial virus in young children in 2015: a systematic review and modelling study. *The Lancet,* 390**,** 946-958.
SIMOES, E. A. 1999. Respiratory syncytial virus infection. *The lancet,* 354**,** 847-852.
SKALSKI, J. H., KOTTOM, T. J. & LIMPER, A. H. 2015. Pathobiology of Pneumocystis pneumonia: life cycle, cell wall and cell signal transduction. *FEMS Yeast Res,* 15.
STEELE, C., MARRERO, L., SWAIN, S., HARMSEN, A. G., ZHENG, M., BROWN, G. D., GORDON, S., SHELLITO, J. E. & KOLLS, J. K. 2003. Alveolar macrophage–mediated killing of Pneumocystis carinii f. sp. muris involves molecular recognition by the dectin-1 β-glucan receptor. *The Journal of experimental medicine,* 198**,** 1677-1688.
STEELE, C., SHELLITO, J. E. & KOLLS, J. K. 2005. Immunity against the opportunistic fungal pathogen Pneumocystis. *Medical mycology,* 43**,** 1-19.
STEPHENS, L. M. & VARGA, S. M. 2020. Function and Modulation of Type I Interferons during Respiratory Syncytial Virus Infection. *Vaccines,* 8**,** 177.
STRINGER, J. R. 2002. Pneumocystis. *International Journal of Medical Microbiology,* 292**,** 391-404.
SUN, Y. & LÓPEZ, C. B. 2017. The innate immune response to RSV: Advances in our understanding of critical viral and host factors. *Vaccine,* 35**,** 481-488.
TABARANI, C. M., BONVILLE, C. A., SURYADEVARA, M., BRANIGAN, P., WANG, D., HUANG, D., ROSENBERG, H. F. & DOMACHOWSKE, J. B. 2013. Novel inflammatory markers, clinical risk factors and virus type associated with severe respiratory syncytial virus infection. *The Pediatric infectious disease journal,* 32**,** e437-e442.
TASAKA, S., KOBAYASHI, S., KAMATA, H., KIMIZUKA, Y., FUJIWARA, H., FUNATSU, Y., MIZOGUCHI, K., ISHII, M., TAKEUCHI, T. & HASEGAWA, N. 2010. Cytokine profiles of bronchoalveolar lavage fluid in patients with pneumocystis pneumonia. *Microbiol Immunol,* 54**,** 425-33.
THOMAS JR, C. F. & LIMPER, A. H. 2004. Pneumocystis pneumonia. *New England Journal of Medicine,* 350**,** 2487-2498.
TOMÁS, A. L., CARDOSO, F., DE SOUSA, B. & MATOS, O. 2020. Detection of anti-Pneumocystis jirovecii antibodies in human serum using a recombinant synthetic multi-epitope kexin-based antigen. *European Journal of Clinical Microbiology & Infectious Diseases,* 39**,** 2205-2209.
TOMÁS, A. L., CARDOSO, F., ESTEVES, F. & MATOS, O. 2016. Serological diagnosis of pneumocystosis: production of a synthetic recombinant antigen for immunodetection of Pneumocystis jirovecii. *Sci Rep,* 6**,** 36287.
TOMÁS, A. L., DE ALMEIDA, M. P., CARDOSO, F., PINTO, M., PEREIRA, E., FRANCO, R. & MATOS, O. 2019. Development of a gold nanoparticle-based lateral-flow immunoassay for pneumocystis pneumonia serological diagnosis at point-of-care. *Frontiers in Microbiology,* 10**,** 2917.
TOMÁS, A. L. & MATOS, O. 2018. Pneumocystis jirovecii pneumonia: Current advances in laboratory diagnosis. *OBM Genetics,* 2**,** 1-29.
TRUONG, J. & ASHURST, J. V. 2023. Pneumocystis Jirovecii Pneumonia. *StatPearls.* Treasure Island (FL): StatPearls Publishing

VARELA, J. M., MEDRANO, F. J., DEI-CAS, E. & CALDERÓN, E. J. 2011. Pneumocystis jirovecii pneumonia in AIDS patients. *Microbes, Viruses and Parasites in AIDS Process. Rijeka: InTech*, 113-42.

VÁZQUEZ, Y., GONZÁLEZ, L., NOGUERA, L., GONZÁLEZ, P. A., RIEDEL, C. A., BERTRAND, P. & BUENO, S. M. 2019. Cytokines in the respiratory airway as biomarkers of severity and prognosis for respiratory syncytial virus infection: an update. *Frontiers in immunology,* 10**,** 1154.

WALZER, P. D. 2001. Pneumocystis carinii infection. *Atlas of Infectious Diseases: Fungal Infections.* Springer.

WANG, M., ZHANG, Z., DONG, X. & ZHU, B. 2023. Targeting β-glucans, vital components of the Pneumocystis cell wall. *Frontiers in Immunology,* 14**,** 1094464.

WANG, S.-H., ZHANG, C., LASBURY, M. E., LIAO, C.-P., DURANT, P. J., TSCHANG, D. & LEE, C.-H. 2008. Decreased inflammatory response in Toll-like receptor 2 knockout mice is associated with exacerbated Pneumocystis pneumonia. *Microbes and infection,* 10**,** 334-341.

WARIS, M. E., TSOU, C., ERDMAN, D. D., ZAKI, S. R. & ANDERSON, L. J. 1996. Respiratory synctial virus infection in BALB/c mice previously immunized with formalin-inactivated virus induces enhanced pulmonary inflammatory response with a predominant Th2-like cytokine pattern. *Journal of Virology,* 70**,** 2852-2860.

WELLIVER, T. P., GAROFALO, R. P., HOSAKOTE, Y., HINTZ, K. H., AVENDANO, L., SANCHEZ, K., VELOZO, L., JAFRI, H., CHAVEZ-BUENO, S., OGRA, P. L., MCKINNEY, L., REED, J. L. & WELLIVER, R. C. 2007. Severe Human Lower Respiratory Tract Illness Caused by Respiratory Syncytial Virus and Influenza Virus Is Characterized by the Absence of Pulmonary Cytotoxic Lymphocyte Responses. *The Journal of Infectious Diseases,* 195**,** 1126-1136.

WELSH, R. M., CHE, J. W., BREHM, M. A. & SELIN, L. K. 2010. Heterologous immunity between viruses. *Immunol Rev,* 235**,** 244-66.

WILEY, J. A. & HARMSEN, A. G. 2008. Pneumocystis Infection Enhances Antibody-Mediated Resistance to a Subsequent Influenza Infection1. *The Journal of Immunology,* 180**,** 5613-5624.

WILLIAMS, A. E., EDWARDS, L., HUMPHREYS, I. R., SNELGROVE, R., RAE, A., RAPPUOLI, R. & HUSSELL, T. 2004. Innate Imprinting by the Modified Heat-Labile Toxin of Escherichia coli (LTK63) Provides Generic Protection against Lung Infectious Disease1. *The Journal of Immunology,* 173**,** 7435-7443.

ZAR, H. J., BARNETT, W., STADLER, A., GARDNER-LUBBE, S., MYER, L. & NICOL, M. P. 2016. Aetiology of childhood pneumonia in a well vaccinated South African birth cohort: a nested case-control study of the Drakenstein Child Health Study. *The Lancet Respiratory Medicine,* 4**,** 463-472.

ZENG, R., CUI, Y., HAI, Y. & LIU, Y. 2012. Pattern recognition receptors for respiratory syncytial virus infection and design of vaccines. *Virus research,* 167**,** 138-145.

ZHANG, N.-N., HUANG, X., FENG, H.-Y., HUANG, L.-N., XIA, J.-G., WANG, Y., ZHANG, Y., WU, X.-J., LI, M., CUI, W. & ZHAN, Q.-Y. 2019. Circulating and Pulmonary T-cell Populations Driving the Immune Response in Non-HIV Immunocompromised Patients with Pneumocystis jirovecii Pneumonia. *International Journal of Medical Sciences,* 16**,** 1221-1230.

Appendix: Buffers and solutions

Western Blot

Separating buffer

- 1.5 M Tris-HCl (pH 8.8)
- 0.4% SDS

Stacking buffer

- 0.5 M Tris-HCl (pH 6.8)
- 0.4% SDS

2x Laemmli sample buffer

- 2.5ml 0.5M Tris (pH 6.8)
- 2.0ml 10% SDS
- 2.0ml Glycerol
- 2.0ml Distilled water
- 1.0ml β-mercaptoethanol
- Bromophenol blue

12.5% gel

- 2.5g Acrylamide (40%)
- 2.0g Separating buffer (pH 8.8)
- 0.75ml Stacking buffer (pH 6.8)
- 3.5ml distilled water
- 3.5µl Tetramethylethylenediamine (TEMED)
- 35µl Ammonium persulphate (APS 10%)

Running buffer

- 30.0g Tris base
- 144.0g Glycine
- 10.0g SDS in 1000ml distilled water

10× Transfer buffer

- 29g Glycine

- 58g Tris Base
- 40µl 10% SDS

Wash buffer

- 50 mM Tris-HCl (pH 8)

Blocking buffer

- 5% bovine serum albumin (BSA)
- 1 × PBS

ELISA wash buffer

- 0.05% Tween 20
- 1 × PBS

Histology

10% Formalin

- 100ml formaldehyde (40% w/v formaldehyde solution)
- 900ml PBS

Dehydration

	Number of changes	Length of Procedure
70% Alcohol	1	30 minutes
96% Alcohol	2	45 minutes
100% Alcohol	4	45 minutes
Xylol	2	60 minutes
Wax (55°to 60°C	2	45 minutes

Rehydration

	Number of changes	Length of Procedure
Xylol	1	3 minutes
Xylol	2	1 minute
Absolute Alcohol	2	1 minute
96% Alcohol	2	1 minute
70% Alcohol	1	1 minute
Water	1	1 minute